

Cellwise outlier detection in heterogeneous populations

Giorgia Zaccaria*

Department of Statistics and Quantitative Methods, University of Milano-Bicocca
and

Luis A. García-Escudero

Department of Statistics and Operational Research, University of Valladolid
and

Francesca Greselin

Department of Statistics and Quantitative Methods, University of Milano-Bicocca
and

Agustín Mayo-Íscar

Department of Statistics and Operational Research, University of Valladolid

September 13, 2024

Abstract

Real-world applications may be affected by outlying values. In the model-based clustering literature, several methodologies have been proposed to detect units that deviate from the majority of the data (rowwise outliers) and trim them from the parameter estimates. However, the discarded observations can encompass valuable information in some observed features. Following the more recent cellwise contamination paradigm, we introduce a Gaussian mixture model for cellwise outlier detection. The proposal is estimated via an Expectation-Maximization (EM) algorithm with an additional step for flagging the contaminated *cells* of a data matrix and then imputing – instead of discarding – them before the parameter estimation. This procedure adheres to the spirit of the EM algorithm by treating the contaminated cells as missing values. We analyze the performance of the proposed model in comparison with other existing methodologies through a simulation study with different scenarios and illustrate its potential use for clustering, outlier detection, and imputation on three real data sets.

Keywords: Robustness, Model-based clustering, Cellwise contamination, Missing data, EM algorithm, Imputation

*Corresponding author: giorgia.zaccaria@unimib.it

1 Introduction

Real data often contain outlying and missing values. In robust statistical literature, several methodologies have been proposed to prevent biased parameter estimates by detecting and downweighting or discarding contaminated cases within a data matrix. These cases typically correspond to entire rows, therefore referred to as rowwise/casewise outliers (Huber, 1964), which are assumed not to follow the distribution of the majority of the data. In recent years, the component-wise contamination model proposed by Alqallaf et al. (2009) has garnered increasing attention from researchers. This introduced a new contamination paradigm that assumes some *cells* of a data matrix have been replaced by arbitrary values. According to it, a low percentage of cellwise contamination potentially corrupts many rows, over all of them, as the number of variables increases. Consequently, casewise trimming would discard valuable information encompassed in the uncontaminated cells of the rows or be unfeasible. In the single-population framework, the cellwise MCD (cellMCD, Raymaekers and Rousseeuw, 2023) represents the most recent proposal for robustly estimating the location and scale parameters in the presence of cellwise contamination, forerunning by the Detection-Imputation (DI) method (Raymaekers and Rousseeuw, 2021) and other methodologies for several purposes, such as principal component analysis (Hubert et al., 2019; see Raymaekers and Rousseeuw, 2024, for a comprehensive review). Both cellMCD and DI, being based on the Expectation-Maximization (EM) algorithm (Dempster et al., 1977), can further handle missing values, faithfully adhering to its spirit by treating contaminated cells as missing information to be imputed. However, they assume one single homogeneous population and cannot deal with heterogeneity in the data, which is common

in practice.

For uncovering contamination in heterogeneous populations, a first class of models has been proposed which accommodate to the presence of outliers by partially relaxing the normality assumption and considering heavy-tailed distributions for the components. This class encompasses the mixture of t distributions (McLachlan and Peel, 2000) and the mixtures of contaminated normal distributions (Punzo and McNicholas, 2016) as examples, both extended to handle Missing At Random (MAR, Rubin, 1976) values in the data by Wang et al. (2004) and Tong and Tortora (2022), respectively, as is common in other statistical methodologies (Little and Rubin, 2019). To deal with contamination in general position in model-based clustering, García-Escudero et al. (2008) introduced TCLUST, which extended the Minimum Covariance Determinant (MCD, Rousseeuw, 1984, 1985) estimator for the location and covariance matrix through the use of classification trimmed likelihoods. Specifically, TCLUST includes a *Concentration* step in the EM algorithm, similar to the C-step in the faster MCD algorithm (FAST-MCD, Rousseeuw and van Driessen, 1999; see also Zhang et al., 2024, for its computationally efficient version in high-dimensional setting), where a certain fraction of observations considered as the most outlying data are removed before the parameter estimation. An analogous trimming approach was considered in a mixture likelihood model-based framework in Neykov et al. (2007) and García-Escudero et al. (2014).

The goal of this paper is to provide a model-based extension of cellMCD in the clustering framework for coping with cellwise contamination and MAR information. The proposal, called cellwise Gaussian Mixture Model (cellGMM), is based upon the maximization of

the log-likelihood via a mixture EM algorithm with a fixed number of components and including constraints to avoid spurious solutions (García-Escudero et al., 2014). The difficult challenge of simultaneously detecting clustering structures via a model-based approach and identifying outlying cells position, influenced by the variable dependence within sub-populations, has been previously addressed by Farcomeni (2014). His snipping proposal for Gaussian mixture models (`sclust`) involves the removal of contaminated cells from the E- and M-step of the algorithm. Nonetheless, `sclust` has some limitations that our proposal attempts to overcome. Indeed, unlike `sclust`, `cellGMM` supplies imputation, say “correction”, for outlying values, as well as for missing values whose positions are known. Additionally, it is able to automatically determine the contamination level in the data matrix. While `sclust` cannot adjust the number of outlying cells within the algorithm after initialization, potentially affecting parameter estimates, `cellGMM` can, as demonstrated in the simulation study presented in Section 3. It is worth noting that the initialization of `cellGMM` is a crucial issue, which we will discuss in Section 2.2 and in detail in the Supplementary Material available online. Other approaches for robust clustering based on cellwise trimming can be found in Farcomeni (2013) and García-Escudero et al. (2021). These approaches are no longer be considered in this work because they do not provide estimators of the component covariance matrices and are essentially based on searching for approximating sets made of G points or G affine sub-spaces in the observed data.

The rest of the paper is organized as follows. We describe our proposal in Section 2, along with its computational aspects. Sections 3 and 4 provide evidence of the `cellGMM` performance compared to other existing methodologies for casewise and cellwise

outlier detection through a simulation study and three real-world applications involving hyperspectral data, image reconstruction and data on cars' features. Finally, a discussion reviews the obtained results and presents open research lines for future investigation in Section 5.

2 Gaussian mixture models with cellwise outliers

The proposed methodology follows in the footsteps of cellMCD by leveraging the EM algorithm in the model-based clustering framework. Consider a p -dimensional random vector drawn from a mixture of G multivariate Gaussian distributions, whose probability density function (pdf) is given by

$$f(\mathbf{x}; \Psi) = \sum_{g=1}^G \pi_g \phi_p(\mathbf{x}; \boldsymbol{\mu}_g, \boldsymbol{\Sigma}_g), \quad (1)$$

where $\phi_p(\cdot; \boldsymbol{\mu}, \boldsymbol{\Sigma})$ is the pdf of the p -variate normal with mean $\boldsymbol{\mu}$ and covariance matrix $\boldsymbol{\Sigma}$. $\Psi = \{\boldsymbol{\pi}, \boldsymbol{\theta}\}$ is the overall parameter set composed of $\boldsymbol{\pi} = \{\pi_g\}_{g=1}^G$ with weights $\pi_g \in (0, 1]$ and such that $\sum_{g=1}^G \pi_g = 1$, and $\boldsymbol{\theta} = \{\boldsymbol{\mu}_g, \boldsymbol{\Sigma}_g\}_{g=1}^G$ with component mean vectors $\boldsymbol{\mu}_g \in \mathbb{R}^p$ and symmetric positive definite component covariance matrices $\boldsymbol{\Sigma}_g \in \mathbb{R}^{p \times p}$.

Let $\mathbf{X} = [x_{ij} : i = 1, \dots, n, j = 1, \dots, p]$ be a data matrix, whose rows $\mathbf{x}_1, \dots, \mathbf{x}_n$, with $\mathbf{x}_i \in \mathbb{R}^p$, are supposed to be a random sample drawn from GMM in (1). It can happen that some individual measurements or cells, i.e., some x_{ij} , have been replaced by outlying values. We refer to the latter as *contaminated* or *unreliable* cells, that can be distributed everywhere throughout the sample. To track their pattern, we define the matrix $\mathbf{W} = [w_{ij} : i = 1, \dots, n, j = 1, \dots, p]$, where $w_{ij} = 1$ if x_{ij} is reliable, and $w_{ij} = 0$

if not because it has been contaminated. We use herein the notation $\mathbf{w}_i, i = 1, \dots, n$, when referring to the rows of \mathbf{W} , but we denote with $\mathbf{W}_{\cdot j}$ the j th column of that matrix (equivalent notation will be used for other matrices considered in this work). According to the values of \mathbf{w}_i , we partition \mathbf{x}_i into $\mathbf{x}_{i[\mathbf{w}_i]}$ and $\mathbf{x}_{i[\mathbf{1}_p - \mathbf{w}_i]}$ (respectively, reliable and unreliable cells in the observation \mathbf{x}_i), where $\mathbf{1}_p$ is a p -dimensional unitary vector. Henceforth, we refer to $\mathbf{1}_p - \mathbf{w}_i$ as \mathbf{w}_i^c for simplicity. In a similar manner, given a vector $\boldsymbol{\mu} \in \mathbb{R}^p$, $\boldsymbol{\mu}_{[\mathbf{w}_i]}$ stands for its sub-vector in $\mathbb{R}^{p[\mathbf{w}_i]}$, where $p[\mathbf{w}_i] = \sum_{j=1}^p w_{ij}$, i.e., the sub-vector corresponding to the cells of \mathbf{x}_i for which $w_{ij} = 1$. Analogously, $\boldsymbol{\Sigma}_{[\mathbf{w}_i, \mathbf{w}_i]}$ symbolizes the $p[\mathbf{w}_i] \times p[\mathbf{w}_i]$ sub-matrix of $\boldsymbol{\Sigma} \in \mathbb{R}^{p \times p}$ obtained by keeping only the rows and columns of $\boldsymbol{\Sigma}$ whose indexes j satisfy $w_{ij} = 1$ in \mathbf{w}_i . Finally, with $\boldsymbol{\mu}_{[j]}$ ($\boldsymbol{\Sigma}_{[j,j]}$) we extract the j th (jj th) element of $\boldsymbol{\mu}$ ($\boldsymbol{\Sigma}$).

Considering the notation introduced, the objective function of the Gaussian Mixture Model with cellwise outliers (cellGMM) to maximize is

$$\ell(\boldsymbol{\Psi}, \mathbf{W}; \mathbf{X}) = \sum_{i=1}^n \ln \left[\sum_{g=1}^G \pi_g \phi_{p[\mathbf{w}_i]}(\mathbf{x}_{i[\mathbf{w}_i]}; \boldsymbol{\mu}_{g[\mathbf{w}_i]}, \boldsymbol{\Sigma}_{g[\mathbf{w}_i, \mathbf{w}_i]}) \right], \quad (2)$$

subject to constraints

$$\|\mathbf{W}_{\cdot j}\|_0 \geq h, \forall j = 1, \dots, p, \quad (3)$$

$$\frac{\max_{g=1, \dots, G} \max_{j=1, \dots, p} \lambda_j(\boldsymbol{\Sigma}_g)}{\min_{g=1, \dots, G} \min_{j=1, \dots, p} \lambda_j(\boldsymbol{\Sigma}_g)} \leq c, \quad (4)$$

where $\lambda_j(\boldsymbol{\Sigma}_g)$ is the j th eigenvalue of the covariance matrix $\boldsymbol{\Sigma}_g$ and $c \geq 1$ is a fixed constant (García-Escudero et al., 2008). The constraint in (3) requires at least h reliable cells in each column, so we set $h \geq 0.75n$ (see Raymaekers and Rousseeuw, 2023). The eigenvalue-ratio constraint in (4) addresses the problem of the unboundedness of (2) and the spurious solutions that may result from its maximization, while maintaining the positive definiteness

of Σ_g .

To solve the constrained maximization in (2), we consider an adaptation of the EM algorithm – typically used for mixture modeling and handling of missingness in the data – which allows to simultaneously detect the outlying cells and find the maximum likelihood estimates of the model parameters. In this EM framework, there are multiple sources of unknown information beyond the model parameters: firstly, the outlying cells of $\{\mathbf{x}_i\}_{i=1}^n$ corresponding to the zeros in $\{\mathbf{w}_i\}_{i=1}^n$, and, secondly, the indicator to the population belonging, also called unit-component membership, reported in $\mathbf{Z} = [z_{ig}, i = 1, \dots, n, g = 1, \dots, G]$, where $z_{ig} = 1$ if the i th observation belongs to the g th component of the mixture, and $z_{ig} = 0$ otherwise. Let \mathbf{z}_i and $\mathbf{x}_{i[\mathbf{w}_i^c]}$ be the “missing” data, and $\mathbf{x}_{i[\mathbf{w}_i]}$ the observed data. The cellGMM complete data log-likelihood is

$$\ell_c(\Psi, \mathbf{W}, \mathbf{Z}; \mathbf{X}) = \sum_{i=1}^n \sum_{g=1}^G z_{ig} \left[\ln(\pi_g) + \ln(\phi_p(\mathbf{x}_{i[\mathbf{w}_i]}, \mathbf{x}_{i[\mathbf{w}_i^c]}; \boldsymbol{\mu}_g, \Sigma_g)) \right] \quad (5)$$

subject to constraints (3) and (4). In the following, we detail the steps of the EM algorithm for the estimation of the cellGMM parameters. The algorithm starts with initial solutions for the parameters, which will be discussed in Section 2.2. The C-step involves estimating \mathbf{W} , whereas the E-step consists of computing expectations of the remaining missing data. In the M-step, we derive the estimates of the overall parameter set Ψ .

Update of \mathbf{W} . At iteration $(t + 1)$, given the current update at iteration t in $\widehat{\Psi}^{(t)}$ and $\mathbf{Z}^{(t)}$, we update the configuration of \mathbf{W} column-by-column. To simplify the notation, we use an intermediate $\widetilde{\mathbf{W}}$ matrix before providing the updated $\mathbf{W}^{(t+1)}$. Consequently, we start from $\widetilde{\mathbf{W}} = \mathbf{W}^{(t)}$ and we update $\widetilde{\mathbf{W}}_{\cdot j}$ sequentially for $j = 1, \dots, p$, by considering the previously estimated $(j - 1)$ columns of $\widetilde{\mathbf{W}}$ as fixed. To this aim, we define the contribution

of the i th observation to the cellGMM objective function in (2) as

$$\ell_{(i)}(\Psi, \mathbf{w}_i; \mathbf{x}_i) = \ln \left[\sum_{g=1}^G \pi_g \phi_{p[\mathbf{w}_i]}(\mathbf{x}_{i[\mathbf{w}_i]}; \boldsymbol{\mu}_{g[\mathbf{w}_i]}, \boldsymbol{\Sigma}_{g[\mathbf{w}_i, \mathbf{w}_i]}) \right]. \quad (6)$$

For the j th column of $\widetilde{\mathbf{W}}$, we compare the contribution of the i th unit to the observed log-likelihood in (6) when we modify the j th element of $\widetilde{\mathbf{w}}_i$ such that its value for i th observation is considered reliable ($w_{ij} = 1$) or contaminated ($w_{ij} = 0$), while the other terms in $\widetilde{\mathbf{w}}_i$ remain unchanged. Therefore, we compute

$$\Delta_{ij} = \ell_{(i)}(\widehat{\Psi}^{(t)}, \widetilde{\mathbf{w}}_i; \mathbf{x}_i, \widetilde{w}_{ij} = 1) - \ell_{(i)}(\widehat{\Psi}^{(t)}, \widetilde{\mathbf{w}}_i; \mathbf{x}_i, \widetilde{w}_{ij} = 0). \quad (7)$$

With the aim of maximizing the observed log-likelihood $\sum_{i=1}^n \ell_{(i)}(\widehat{\Psi}^{(t)}, \mathbf{w}_i; \mathbf{x}_i)$ subject to constraint (3), we attain the optimum by setting $\widetilde{w}_{ij} = 1$ for all indexes i corresponding to the h largest values of $\{\Delta_{ij}\}_{i=1}^n$, 0 otherwise. Repeating this procedure for all columns of $\widetilde{\mathbf{W}}$ we obtain $\mathbf{W}^{(t+1)} = \widetilde{\mathbf{W}}$. As shown in Raymaekers and Rousseeuw (2023), the chosen order for the update of \mathbf{W} does not seem to significantly affect the performance of the procedure.

Update of \mathbf{Z} and $\mathbf{X}_{[\mathbf{w}^c]}$. At iteration $(t + 1)$, we update the membership matrix \mathbf{Z} and the unreliable data in \mathbf{X} corresponding to the zero elements into $\mathbf{W}^{(t+1)}$. Therefore, we consider the outlying cells uncovered in $\mathbf{W}^{(t+1)}$ as missing values. We compute the expected value of the complete data log-likelihood in (5) conditional on the observed and reliable data, given $\mathbf{W}^{(t+1)}$ and the current estimate of the parameter set in $\widehat{\Psi}^{(t)}$, i.e.

$\mathbb{E}[\ell_c(\Psi, \mathbf{W}^{(t+1)}, \mathbf{Z}; \mathbf{X}) | \mathbf{X}_{[\mathbf{w}^{(t+1)}]}; \widehat{\Psi}^{(t)}]$, as follows

$$Q(\Psi; \widehat{\Psi}^{(t)}) = \sum_{i=1}^n \sum_{g=1}^G \mathbb{E}[Z_{ig} | \mathbf{x}_{i[\mathbf{w}_i^{(t+1)}]}; \widehat{\Psi}^{(t)}] \times \left\{ \ln(\pi_g) - \frac{1}{2} \left[\ln(|\Sigma_g|) + \text{tr}(\Sigma_g^{-1} \right. \right. \\ \left. \left. \mathbb{E} \left[\left((\mathbf{x}'_{i[\mathbf{w}_i^{(t+1)}]}, \mathbf{X}'_{i[\mathbf{w}_i^{(t+1)}c_1]} - \boldsymbol{\mu}_g) \right) \left((\mathbf{x}'_{i[\mathbf{w}_i^{(t+1)}]}, \mathbf{X}'_{i[\mathbf{w}_i^{(t+1)}c_1]} - \boldsymbol{\mu}_g) \right)' | \mathbf{x}_{i[\mathbf{w}_i^{(t+1)}]}, z_{ig} = 1; \widehat{\Psi}^{(t)} \right] \right] \right\}, \quad (8)$$

where we omit the constant term of the normal distribution not depending on the model parameters. The computation of all the conditional expectations required in (8) is reported in Section 1.1 of the Supplementary Material. These expectations constitute the E-step of the proposed algorithm, while the M-step maximizes $Q(\Psi; \widehat{\Psi}^{(t)})$ with respect to Ψ by updating the estimates of the cellGMM parameters. The latter correspond to the usual estimates of the GMM parameters computed on the *completed* data $\left\{ \left\{ \tilde{\mathbf{x}}_{i(g)}^{(t+1)} = (\mathbf{x}_{i[\mathbf{w}_i^{(t+1)}]}, \widehat{\mathbf{x}}_{i[\mathbf{w}_i^{(t+1)}c_1]^{(g)}}) \right\}_{g=1}^G \right\}_{i=1}^n$ (see Section 1.1 of the Supplementary Material for details).

2.1 Penalized log-likelihood approach for cellGMM

The EM algorithm described for estimating the cellGMM parameters uncovers a fixed number h of hopefully reliable cells per variable through \mathbf{W} . However, the cellwise outlier contamination can differently affects the variables. To prevent excessive cell flagging, we add penalty terms to the log-likelihood in (2) as follows

$$\ell_{\text{pen}}(\Psi, \mathbf{W}; \mathbf{X}) = \sum_{i=1}^n \ln \left[\sum_{g=1}^G \pi_g \phi_{p[\mathbf{w}_i]}(\mathbf{x}_{i[\mathbf{w}_i]}; \boldsymbol{\mu}_{g[\mathbf{w}_i]}, \Sigma_{g[\mathbf{w}_i, \mathbf{w}_i]}) \right] - \sum_{j=1}^p \sum_{i=1}^n q_{ij} (1 - w_{ij}), \quad (9)$$

where $\mathbf{Q} = [q_{ij} : i = 1, \dots, n, j = 1, \dots, p]$ represents a tuning matrix (see Section 2.2 for the details on its setting). Maximizing (9) under constraints (3) and (4) can avoid detecting an unnecessary high number of contaminated cells for an appropriate \mathbf{Q} matrix.

It is worth noting that the penalty term plays a crucial role in the update of \mathbf{W} , while it can be ignored in the other steps of the cellGMM algorithm. Specifically, the penalized version of the C-step is described below.

Penalized update of \mathbf{W} . Inspired by the rationale in Raymaekers and Rousseeuw (2023), we propose a modified Δ_{ij} , denoted as $\tilde{\Delta}_{ij}$, which is defined from

$$\tilde{\ell}_{(i)}(\Psi, \mathbf{w}_i, \mathbf{z}_i; \mathbf{x}_i) = \sum_{g=1}^G z_{ig} \left[\ln(\pi_g) + \ln(\phi_{p[\mathbf{w}_i]}(\mathbf{x}_{i[\mathbf{w}_i]}; \boldsymbol{\mu}_{g[\mathbf{w}_i]}, \boldsymbol{\Sigma}_{g[\mathbf{w}_i, \mathbf{w}_i]}) \right] - \sum_{j=1}^p q_{ij}(1 - w_{ij}), \quad (10)$$

as

$$\begin{aligned} \tilde{\Delta}_{ij} &= \tilde{\ell}_{(i)}(\hat{\Psi}^{(t)}, \tilde{\mathbf{w}}_i, \mathbf{z}_i^{(t)}; \mathbf{x}_i, \tilde{w}_{ij} = 1) - \tilde{\ell}_{(i)}(\hat{\Psi}^{(t)}, \tilde{\mathbf{w}}_i, \mathbf{z}_i^{(t)}; \mathbf{x}_i, \tilde{w}_{ij} = 0) \\ &= -\frac{1}{2} \left\{ \sum_{g=1}^G z_{ig}^{(t)} \left[\ln(\hat{C}_{ij(g)}) + \frac{(x_{ij} - \hat{x}_{ij(g)})^2}{\hat{C}_{ij(g)}} \right] + \ln(2\pi) \right\} + q_{ij}, \end{aligned} \quad (11)$$

where $\hat{x}_{ij(g)} = \hat{\boldsymbol{\mu}}_{g[j]}^{(t)} + \hat{\boldsymbol{\Sigma}}_{g[j, \tilde{\mathbf{w}}_i]}^{(t)} (\hat{\boldsymbol{\Sigma}}_{g[\tilde{\mathbf{w}}_i, \tilde{\mathbf{w}}_i]}^{(t)})^{-1} (\mathbf{x}_{i[\tilde{\mathbf{w}}_i]} - \hat{\boldsymbol{\mu}}_{g[\tilde{\mathbf{w}}_i]}^{(t)})$ and $\hat{C}_{ij(g)} = \hat{\boldsymbol{\Sigma}}_{g[j, j]}^{(t)} - \hat{\boldsymbol{\Sigma}}_{g[j, \tilde{\mathbf{w}}_i]}^{(t)} (\hat{\boldsymbol{\Sigma}}_{g[\tilde{\mathbf{w}}_i, \tilde{\mathbf{w}}_i]}^{(t)})^{-1} \hat{\boldsymbol{\Sigma}}_{g[\tilde{\mathbf{w}}_i, j]}^{(t)}$ are the expectation and the variance, respectively, of the cell X_{ij} for the g th mixture component conditional on the reliable cells in the same row i , excluding the j th variable. We obtain this result thanks to the additive property of the Mahalanobis distance and log-likelihood reported in Raymaekers and Rousseeuw (2023, Proposition 5), which stem from the Gaussian distribution properties.

In this case, the update of $\tilde{\mathbf{W}}_{.j}$, and precisely the number of cells flagged as outliers, depends on the values of $\tilde{\Delta}_{ij}$: a) if the number of nonnegative $\tilde{\Delta}_{ij}$ is *greater than* h , i.e., $\#\{\tilde{\Delta}_{ij} \geq 0\} > h$, we set to one the corresponding cells \tilde{w}_{ij} for which $\tilde{\Delta}_{ij} \geq 0$, and to zero the others; b) if the number of nonnegative $\tilde{\Delta}_{ij}$ is *lower than or equal to* h , i.e., $\#\{\tilde{\Delta}_{ij} \geq 0\} \leq h$, we set to one the cells \tilde{w}_{ij} corresponding to the h highest $\tilde{\Delta}_{ij}$, and to

zero the other cells. Consequently, a higher number of cells can be considered as reliable in scenario a), whereas this number is h in scenario b). The penalized log-likelihood approach aims to enable the cellGMM algorithm to recover cells *wrongly* flagged by the unpenalized cellGMM, potentially improving estimation accuracy, as we will see in Section 3.

2.2 Computational issues

Initialization. In the implementation of the EM-type algorithm for estimating the cellGMM parameters, their initialization is pivotal. In Section 1.2 of the Supplementary Material, we detail the procedure proposed to obtain initial solutions for \mathbf{W} and Ψ , along with the tuning parameters' setting used in our experiments. The initialization involves applying TCLUS_T individually to each variable and pairs of variables with a fixed trimming level for the initial solution of \mathbf{W} and computing TCLUS_T on random subsets of variables, followed by a trimmed k -means (Cuesta-Albertos et al., 1997) type algorithm to obtain the initial solution for Ψ . The provided procedure has proved to be compelling aligning closely with the rationale underlying cellGMM. Nonetheless, alternative approaches could be implemented to tackle this issue, that remains open for future work.

Missing information. The cellGMM algorithm can be used when data are affected by missing information. Specifically, the cells of \mathbf{W} corresponding to the missing values in \mathbf{X} are set to 0, and the update of \mathbf{W} is computed only on the observed cells.

Convergence in the target function. The convergence of the cellGMM algorithm is evaluated through the Aitken acceleration-based stopping criterion (McLachlan and Krishnan, 2008, pp. 142-144).

Setting of the penalization tuning matrix \mathbf{Q} . Following Raymaekers and Rousseeuw (2023), we set the generic element of \mathbf{Q} as

$$q_{ij} = \frac{1}{2} \left[\sum_{g=1}^G \hat{z}_{ig} \ln \left(\frac{1}{(\hat{\Sigma}_g^{-1})_{[j,j]}} \right) + \chi_{1,1-\alpha}^2 + \ln(2\pi) \right], \quad (12)$$

where \hat{z}_{ig} and $\hat{\Sigma}_g$ are the estimates obtained at convergence by cellGMM with no penalty (i.e., $\mathbf{Q} = \mathbf{0}$), and $\chi_{1,1-\alpha}^2$ is the quantile of the chi-squared distribution with one degree of freedom and probability $1 - \alpha$ ($\alpha = 0.01$ in our experiments). As we will show in Section 3, the use of the penalized log-likelihood approach for cellGMM usually increases its effectiveness.

3 Simulation study

We carry out herein a simulation study to assess the performance of cellGMM in clustering and parameter estimation recovery. We generate random samples from (1) by considering three scenarios: *Scenario 1* and *Scenario 2* with $n = 200, p = 5, G = 2$, non-spherical with $\Sigma_1 = \Sigma_2 = [\sigma_{ii} = 1, \sigma_{ij} = 0.9^{|i-j|}, i, j = 1, \dots, p, i \neq j]$, unbalanced ($\boldsymbol{\pi} = [0.3, 0.7]$), and well-separated and close components, respectively; *Scenario 3* with $n = 400, p = 15, G = 4$, non-spherical (equal to Scenario 1 and 2 with 4 components), unbalanced ($\boldsymbol{\pi} = [0.2, 0.2, 0.3, 0.3]$), and well-separated components. The components' configuration is controlled through the overlapping measure ω introduced by Maitra and Melnykov (2010), where well-separated and close components correspond to $\omega_{\max} < 0.01$ and $0.05 < \omega_{\max} < 0.06$, respectively. For each scenario, we obtain 100 data matrices that we contaminate with 0%, 5% and 10% of outliers randomly drawn from a uniform

Table 1: Number of samples on which each model can be properly computed (# samp.), mean of the Misclassification Rate (mMR), Mean Squared Error (MSE) of the component mean vectors and Kullback-Leibler (KL) discrepancy for the component covariance matrices per scenario, percentage of contamination, and model

% out.	Model	Scenario 1						Scenario 2						Scenario 3									
		# samp.	mMR	MSE $_{\mu_1}$	MSE $_{\mu_2}$	KL $_{\Sigma_1}$	KL $_{\Sigma_2}$	# samp.	mMR	MSE $_{\mu_1}$	MSE $_{\mu_2}$	KL $_{\Sigma_1}$	KL $_{\Sigma_2}$	# samp.	mMR	MSE $_{\mu_1}$	MSE $_{\mu_2}$	MSE $_{\mu_3}$	MSE $_{\mu_4}$	KL $_{\Sigma_1}$	KL $_{\Sigma_2}$	KL $_{\Sigma_3}$	KL $_{\Sigma_4}$
0	cellGMM.pen0	100	0.02	0.02	0.01	2.22	2.07	100	0.12	0.09	0.03	2.62	2.29	100	0.00	0.02	0.02	0.01	0.01	9.60	9.60	9.22	9.27
	cellGMM.penb	100	0.00	0.01	0.01	0.35	0.22	100	0.06	0.04	0.01	0.58	0.30	100	0.00	0.01	0.01	0.01	0.01	2.43	2.40	1.96	2.00
	TCLUST	100	0.00	0.05	0.01	1.34	0.42	100	0.05	0.07	0.02	1.43	0.48	100	0.00	0.02	0.02	0.01	0.02	2.80	2.87	2.01	2.08
	schust_25	98	0.03	0.43	0.33	1.54	5.99	100	0.22	0.35	0.08	2.71	2.16	0									
	MNM	100	0.00	0.01	0.01	0.26	0.11	100	0.05	0.07	0.02	0.46	0.18	100	0.00	0.01	0.01	0.01	0.01	1.63	1.59	1.08	1.08
	MCNM	100	0.00	0.01	0.01	0.29	0.14	100	0.05	0.07	0.03	0.48	0.22	100	0.00	0.01	0.01	0.01	0.01	1.65	1.60	1.09	1.08
	MM	100	0.00	0.01	0.01	0.26	0.11	100	0.05	0.07	0.02	0.44	0.19	100	0.00	0.01	0.01	0.01	0.01	1.64	1.59	1.08	1.08
	5	cellGMM.pen0	100	0.03	0.03	0.01	1.93	1.69	100	0.17	0.11	0.07	2.73	2.03	100	0.00	0.02	0.02	0.01	0.01	8.88	8.88	8.01
cellGMM.penb		100	0.02	0.02	0.01	0.48	1.69	100	0.11	0.07	0.02	1.07	0.40	100	0.00	0.01	0.01	0.01	0.01	2.95	2.96	2.19	2.22
TCLUST		100	0.07	0.03	0.01	0.41	0.16	100	0.11	0.03	0.01	0.53	0.21	100	0.55	8.51	7.31	3.62	3.36	654.45	652.95	412.24	458.15
schust_25		97	0.06	0.82	0.60	8.96	10.30	94	0.25	0.20	0.10	3.48	2.93	0									
schust_5		93	0.02	0.08	0.03	16.85	7.97	90	0.18	0.09	0.07	5.59	2.43	90	0.03	0.72	1.08	0.17	0.18	119.21	80.63	74.56	70.52
MNM		100	0.10	0.60	0.02	165.18	31.78	100	0.38	0.79	0.24	321.81	21.66	100	0.04	0.36	0.24	0.12	0.18	289.70	434.74	340.51	402.84
MCNM		100	0.09	0.03	0.01	1.48	0.29	100	0.36	0.97	0.24	234.98	7.64	100	0.08	0.05	0.05	0.02	0.03	40.42	56.21	26.58	33.83
MM		100	0.08	0.03	0.01	3.89	0.45	100	0.35	1.00	0.20	294.39	5.34	100	0.13	0.44	0.04	0.02	0.16	136.48	56.89	25.13	58.92
10	cellGMM.pen0	100	0.05	0.04	0.01	1.73	1.17	100	0.18	0.11	0.07	2.68	1.55	100	0.03	2.28	0.02	0.02	0.03	12.92	7.65	6.24	6.18
	cellGMM.penb	100	0.04	0.03	0.01	0.66	5.23	100	0.14	0.09	0.04	1.47	0.51	100	0.03	1.54	0.01	0.03	0.02	10.55	8.02	6.42	4.53
	TCLUST	100	0.22	0.73	0.02	96.25	4.68	100	0.47	1.37	0.56	62.53	49.53	100	0.64	8.40	6.65	4.75	4.11	869.52	922.00	928.54	889.80
	schust_25	93	0.07	0.47	0.44	19.94	19.08	88	0.24	0.16	0.09	3.88	3.29	0									
	schust_10	88	0.03	0.33	0.09	35.62	16.86	63	0.21	0.16	0.08	9.00	4.02	53	0.15	2.66	2.33	0.64	1.05	265.28	103.75	141.24	128.33
	MNM	100	0.18	0.99	0.05	322.35	48.78	100	0.50	1.06	0.66	129.08	259.42	100	0.14	1.23	1.03	0.47	0.83	600.04	870.91	696.80	817.54
	MCNM	100	0.13	0.05	0.01	10.18	0.92	100	0.42	0.91	0.28	282.24	26.70	100	0.24	1.62	0.69	0.21	0.46	208.39	253.67	157.00	228.96
	MM	100	0.13	0.06	0.02	46.44	2.73	100	0.41	0.86	0.25	318.90	42.47	100	0.32	3.66	1.62	0.35	1.23	565.00	368.90	211.09	446.74

distribution in the interval $[-10, 10]$, ensuring they do not lie within the 99th percentile ellipsoid of any component. Therefore, we consider 900 random samples altogether. Six additional scenarios with missing data and more extreme contamination are reported in the Supplementary Material.

First, we apply cellGMM without any penalty (cellGMM.pen0). Afterward, we run the penalized version of the algorithm (cellGMM.penb) with the same initialization, using the penalty defined in (12), which is derived from the parameters estimated at the convergence

Table 2: Statistics on outlier detection and imputation: percentage of True Positive and False Positive (%TP and %FP), Mean Absolute Error (MAE) and Root Mean Squared Error (RMSE) for comparing the original and imputed data matrices per scenario, percentage of contamination, and model

% out.	Method	Scenario 1				Scenario 2				Scenario 3			
		%TP	%FP	MAE	RMSE	%TP	%FP	MAE	RMSE	%TP	%FP	MAE	RMSE
0	cellGMM.pen0	25.00	0.22	0.55		25.00	0.21	0.46		25.00	0.20	0.44	
	cellGMM.penb	2.26	0.02	0.15		3.31	0.04	0.20		2.78	0.03	0.16	
	TCLUST	25.00				25.00				25.00			
	sclust_25	25.00				25.00							
	MCNM	6.38				4.57				40.69			
	MtM	26.05				25.14				25.12			
	cellMCD	13.76	0.51	1.47		2.17	0.02	0.18		5.52	0.30	1.39	
	DI	12.66	0.46	1.36		1.93	0.02	0.19		15.24	0.68	1.91	
5	cellGMM.pen0	96.20	21.25	0.24	0.68	97.30	21.19	0.22	0.51	96.64	21.23	0.22	0.56
	cellGMM.penb	96.56	3.56	0.10	0.56	96.80	5.37	0.10	0.40	95.47	3.78	0.06	0.29
	TCLUST	99.56	21.08			99.66	21.07			54.65	23.44		
	sclust_25	71.61	22.55			92.36	21.45						
	sclust_5	54.67	2.39			77.71	1.17			45.64	2.86		
	MCNM	93.58	17.29			57.02	10.28			75.33	35.55		
	MtM	99.54	36.48			59.86	32.31			92.51	48.36		
	cellMCD	94.20	13.71	0.53	1.49	96.76	2.20	0.05	0.23	92.18	3.87	0.22	1.10
DI	92.12	5.29	0.19	0.64	96.78	1.97	0.05	0.24	90.03	12.37	0.57	1.68	
10	cellGMM.pen0	94.98	17.22	0.29	0.89	95.47	17.17	0.22	0.55	93.47	17.39	0.29	0.84
	cellGMM.penb	94.31	6.31	0.20	0.84	94.87	6.33	0.15	0.52	92.01	6.13	0.17	0.68
	TCLUST	64.94	20.56			65.35	20.52			44.14	22.87		
	sclust_25	70.30	19.97			89.45	17.84						
	sclust_10	59.12	4.54			78.97	2.34			48.88	5.68		
	MCNM	92.77	31.86			50.94	16.14			70.27	45.49		
	MtM	96.21	40.92			60.56	34.19			77.39	52.65		
	cellMCD	89.46	13.32	0.68	1.82	94.62	2.07	0.07	0.28	88.55	3.28	0.21	1.00
DI	89.45	2.53	0.12	0.49	94.67	1.92	0.07	0.28	88.56	5.68	0.28	1.06	

of the unpenalized cellGMM. The proposed methodology is also compared with those illustrated in Section 1: i) TCLUST (R package `tclust`) with 25% of contamination, where the trimmed units are assigned a posteriori to the components; ii) sclust (R package `snipEM`) with the suggested initialization for \mathbf{W} by considering 25% and the true percentage of outliers per variable; iii-v) Multivariate Normal Mixture (MNM), Multivariate Contaminated Normal Mixture (MCNM) and Multivariate t Mixture with 25% of contamination (MtM),

which are implemented in the R package `MixtureMissing`. The classification performance of the models is evaluated through the Misclassification Rate, while the recovery of the parameters is assessed via the Mean Squared Error for the component mean vectors and the Kullback-Leibler discrepancy for the component covariance matrices (see the Supplementary Material for additional evaluation indices). To correctly compute the latter, we need to solve the label switching problem. With this aim, we order the estimated components via the complete likelihood-based labelling method introduced by Yao (2015). The results reported in Table 1 show that the penalized version of cellGMM usually outperforms the unpenalized one, especially when the number of variables is higher and the components are well-separated (Scenario 3). In this case, cellGMM benefits from the relationships among variables in the imputation of the outlying cells, which in turn affects the parameter estimates, unlike `sclust` which trims them out. Additionally, the higher the contamination level, the greater the difference between cellGMM.penb and the methodologies for rowwise outlier detection, i.e., TCLUS, MCNM and *MtM*, or the non-robust GMM, i.e. MNM. This is due to the fact that cellwise outliers spread out through the observations as the contamination level increases. Therefore, they can affect more than half of the rows, leading to severely biased parameter estimates, even for methods like TCLUS (see the results for 10% of contamination in Table 1).

To address the correct detection of outliers and data matrix imputation, we compute the percentage of True and False Positives on one hand, and the Mean Absolute Error and Root Mean Squared Error between the original and imputed data matrices on the other hand. To this aim, we also consider cellMCD and DI from the R package `cellWise`. For

the model-based clustering methodologies with rowwise outlier detection, we build a \mathbf{W} matrix by setting to zero all the cells of the rows that have been flagged as contaminated. Table 2 illustrates the results. In this case as well, the penalized version of cellGMM outperforms the unpenalized one in detecting the unreliable cells, with a drastic decrease in the percentage of false positives and a slight decrease in the true positive due to the enlarged number of cells flagged in cellGMM.pen0 by constraint. The accurate identification of outliers is reflected in enhanced values for the indices assessing the imputation of contaminated cells, with improvements between cellGMM.pen0 and cellGMM.penb. Due to this better performance, we report the results of cellGMM.penb directly in Section 4.

In Table 2, the difference between the proposal and the model-based clustering methodologies sharpens as the contamination level increases and components overlap, up to the higher-dimensional case (Scenario 3), where cellGMM generally outperforms the competitors significantly. The single-population methods have better results in Scenario 2 with close components, as expected, since it is more likely that the components are so overlapping that they appear as a single population. In contrast, their performance worsens in Scenario 1 and Scenario 3, both in terms of %TP and %FP. However, it is worth noting that in Scenario 1 with 10% of contamination, DI has lower %FP and imputation indices than cellGMM, despite having a lower %TP. This is riskier for a robust model since the failure to detect outliers can heavily affect the parameter estimates. The peculiar behavior of cellGMM compared to DI in Scenario 1 with 10% of contamination, especially in the imputation results, is due to a higher misclassification rate of the former, which can favor DI over cellGMM. Indeed, if the components are well-separated and a unit is misclassified,

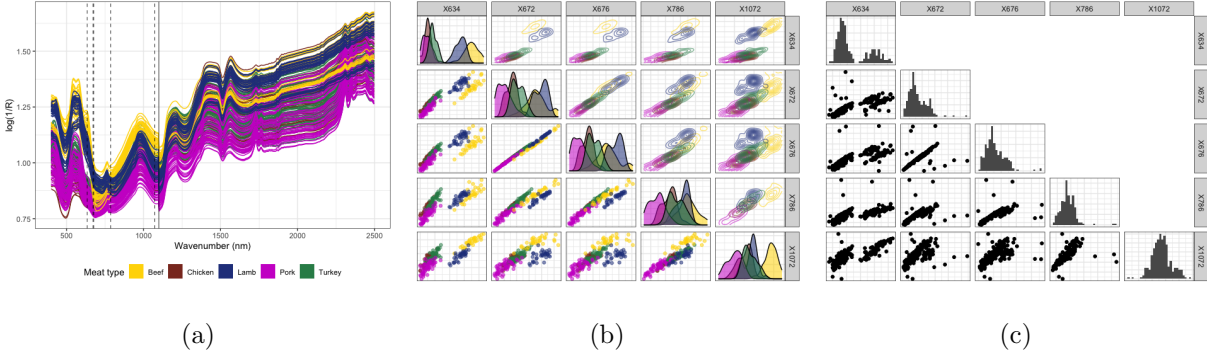


Figure 1: Homogenized Meat data set. (a) Visible and near infrared spectra of five homogenized meat types (dashed lines: selected wavelengths; solid line: discontinuity); (b) Pair plot of the original data: true classification in five homogenized meat types; (c) Pair plot of the data with 3% of contamination.

the imputation within the wrong component is worse than the DI’s imputation between the two components. The additional scenarios illustrated in the Supplementary Material provide further insights into the performance of cellGMM and its competitors.

4 Real data examples

4.1 Homogenized Meat Data Set

Near-infrared reflectance spectroscopy is a method often used for collecting data in food authenticity studies (Downey, 1996, among others) since it is able to discern the properties and, therefore, the nature of food samples. In this section, we analyze the homogenized meat data set presented by McElhinney et al. (1999) to evaluate the cellGMM performance in correctly classifying the samples from their visible and infra-red spectra. For each

Table 3: Misclassification rate comparing the theoretical and the estimated classification of meat samples in two classes per model and percentage of contamination and missing values, i.e. $(a\%, b\%)$

	cellGMM	TCLUST	sclust	MNM	MCNM	MtM
(0%, 0%)	0.01	0.00	0.00	0.00	0.00	0.00
(3%, 0%)	0.01	0.03	0.04	0.05	0.05	0.06
(3%, 2%)	0.01	-	-	0.05	0.06	0.06
(10%, 0%)	0.02	0.16	0.07	0.15	0.25	0.20

of the 231 homogenized meat samples 1050 reflectance measurements are collected with wavelengths between 400 nm and 2500 nm at 2 nm intervals. Due to the number of measurements, one of the first tasks to handle is to reduce the dimensionality of the data. Methods for variable selection were applied on this data set by Murphy et al. (2010) and, in a robust framework, by Cappozzo et al. (2021). We refer to the latter by considering five relevant wavelengths which span the protein spectral region: the first four belonging to the visible part of the spectrum (634 nm, 672 nm, 676 nm and 786 nm) and the remaining one within the near-infrared part (1072 nm). In Figures 1a-1b, we display the selected wavelengths. It is worth noticing that, even if the original classes are five (beef, chicken, lamb, pork, turkey), some of the selected variables, such as the wavelengths 634 nm and 676 nm, turn out to be important to distinguish red meats (beef and lamb) from white meats (chicken, pork and turkey). This evidence was also highlighted by Murphy et al. (2010) and can be seen in Figure 1b as well. Therefore, we consider the classification of samples in two classes and randomly adulterate them via 3% (without and with 2% of missing) and 10% of cellwise contamination in the range $[0.73, 1.25]$ (see Figure 1c as an example).

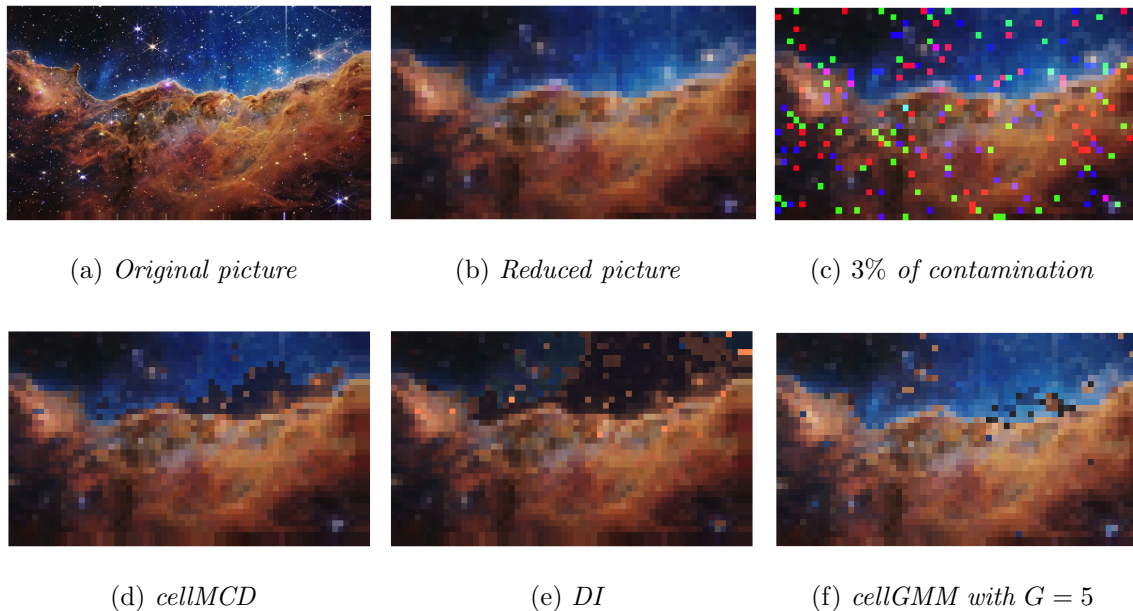


Figure 2: Carina Nebula birth. The methods’ imputation are shown in (d)-(f).

We run cellGMM and sclust with the theoretical level of contamination, except in the case where no missing data or outliers are introduced, in which case the contamination level is set to 0.01. TCLUST, MNM, MCNM, and MtM are all run with the same settings used in the simulation study. As reported in Table 3, as the level of contamination increases, the performance gap between cellGMM and its competitors becomes evident. Indeed, with 10% of contamination, cellGMM maintains good classification results, while the performance of the competitors deteriorates. Additional results can be found in Section 3.1 of the Supplementary Material.

4.2 Carina Nebula Data Set

The proposed methodology is also suitable for image reconstruction. In this framework, we evaluate the detection and “correction” of contaminated cells through their imputation.

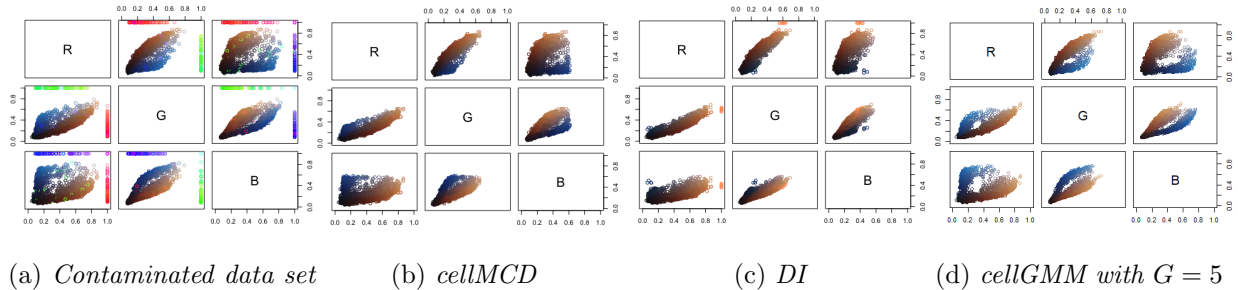


Figure 3: Pair plots of the Carina Nebula data set. The methods’ imputation are shown in (b)-(d).

Specifically, we analyze an image captured by the James Webb Space Telescope, which depicts the edge of NGC 3324 located in the northwest corner of the Carina Nebula. The image of the stars’ birth is available at <https://science.nasa.gov/universe/stars/>. The original picture has 1600×927 pixels (Figure 2a), corresponding to more than one million units measured in three variables (RGB). Due to its high size, we reduce it into 60×35 pixels (Figure 2b), which we then corrupt with 3% of contamination, as depicted in Figures 2c and 3a.

Given our goal, the most appropriate methods to compare to cellGMM are cellMCD and DI, as they provide imputation for contaminated cells. As shown in Figures 2d-2f and 3b-3d, cellGMM demonstrates better potential in image reconstruction than the single-population methods. Moreover, as expected, the higher the number of components, the better the classification performance of cellGMM. This is evident by considering the RMSE between the imputed and the original data sets, which is 0.073 for cellGMM with $G = 2$ and 0.059 for cellGMM with $G = 5$, both lower than 0.079 for cellMCD and 0.127 for DI.

Table 4: Ten representative cars per cluster

Cluster 1	Cluster 2	Cluster 3	Cluster 4
Audi A4	Chevrolet Spark	Aston Martin DB9	BMW X5
Jaguar XF Sportbrake	Hyundai i10	Aston Martin DB9 Volante	BMW X6
Kia Optima	Kia Picanto	Aston Martin V12 Zagato	Hyundai i800
Lexus GS	Peugeot 107	Aston Martin Vanquish	Jeep Grand Cherokee
Mercedes-Benz E-Class Coupé	Proton Savvy	Aston Martin Vantage	Land Rover Discovery 4
Skoda Octavia	SEAT Mii	Aston Martin Vantage Roadster	Land Rover Range Rover
Vauxhall Cascada	Suzuki Alto	Audi R8	Mercedes-Benz G-Class
Vauxhall Insignia Sports Tourer	Toyota AYGO	Audi R8 V10	Mercedes-Benz GL-Class
Volkswagen CC	Toyota iQ	Bentley Continental	Porsche Cayenne
Volkswagen Passat	Volkswagen Up	Bentley Continental GTC	Toyota Land Cruiser V8

4.3 Top Gear Data Set

In this section, we analyze the car data set available in the R package `robustHD` (Alfons, 2021), called *TopGear*, which contains authentic missing values (2.74% of the cells) and potential outliers. We focus on the eleven numerical variables by removing the two cars with more missing than observed values, resulting in a final sample size of $n = 295$, and transforming the highly skewed variables using their logarithms, as reported in Raymaekers and Rousseeuw (2023). Unlike these authors, we provide a cluster-oriented approach to this data set by setting $G = 4$, which identifies meaningful groups with distinct features. The cars are divided into “compact and mid-size sedans and crossovers” (Cluster 1); “economy and city cars” (Cluster 2); “luxury and high-performance cars” (Cluster 3); “large SUVs and off-roaders” (Cluster 4). A list of ten representative cars per cluster, selected as those with the highest posterior probabilities, is provided in Table 4, while a comprehensive overview of the clusters is reported in Section 3.2 of the Supplementary Material.

All the variables are affected by unreliable cells, particularly *Weight* (17.63%), *Width* (11.86%), *Length* (11.19%), *Height* (11.19%), *MPG* (8.47%), and $\ln(\text{Price})$ (8.14%). For

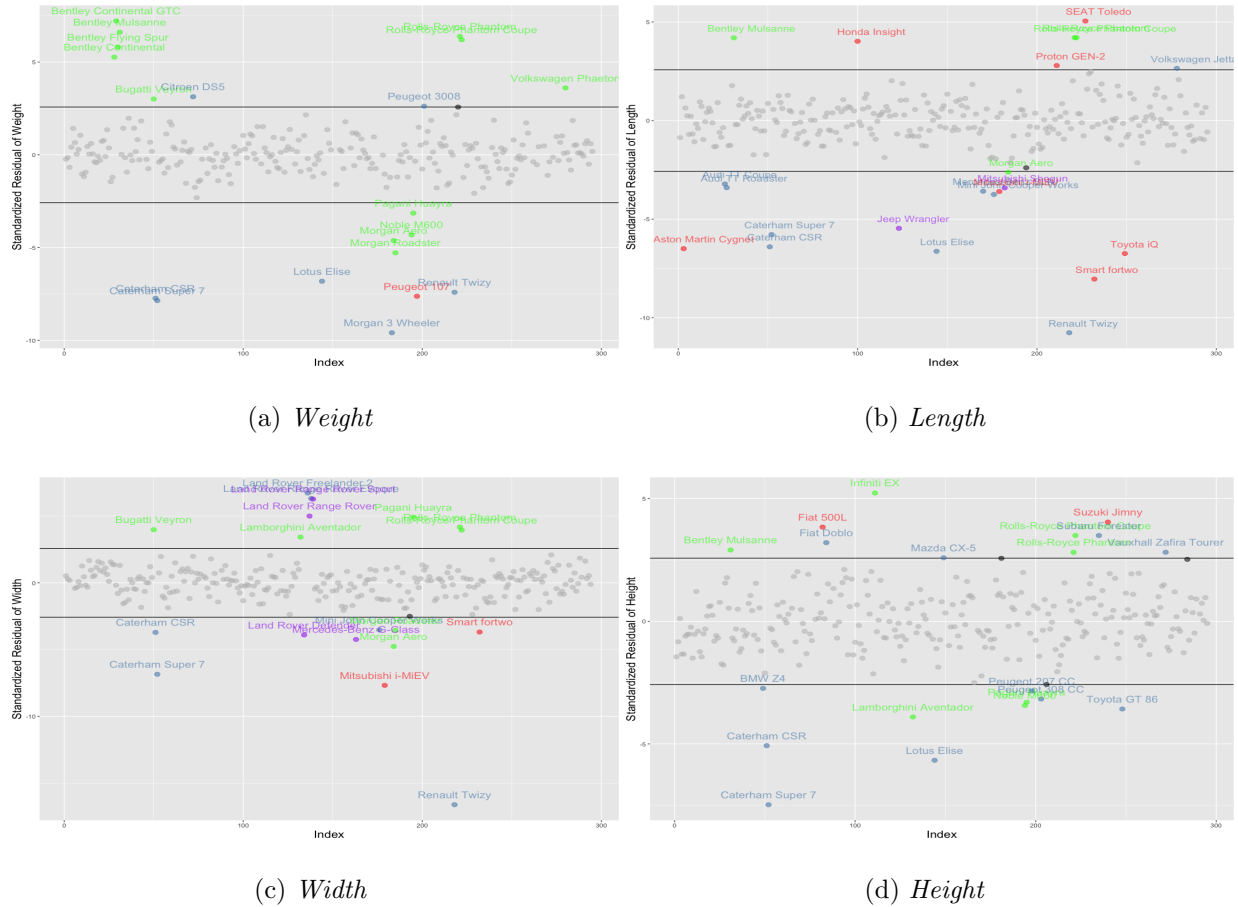
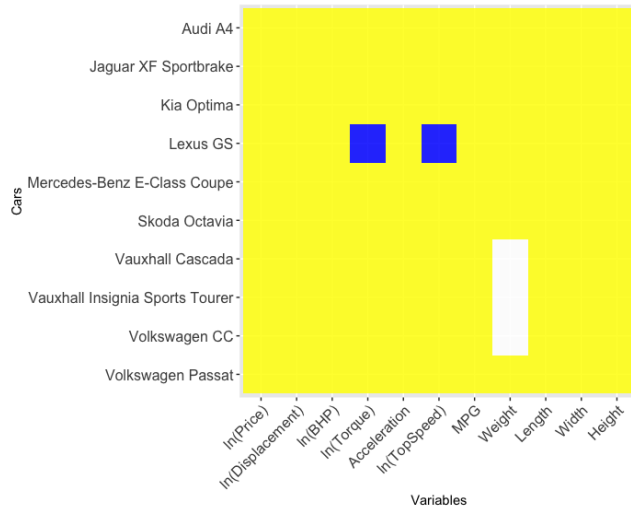
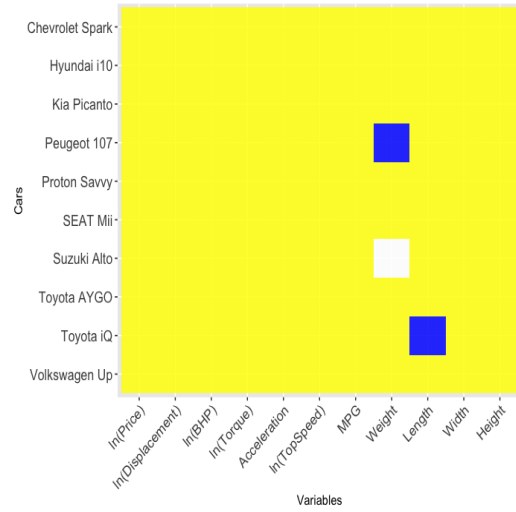


Figure 4: Top Gear data set: index plot of the standardized residuals per variable (Cluster 1: blue; Cluster 2: red; Cluster 3: green; Cluster 4: purple)

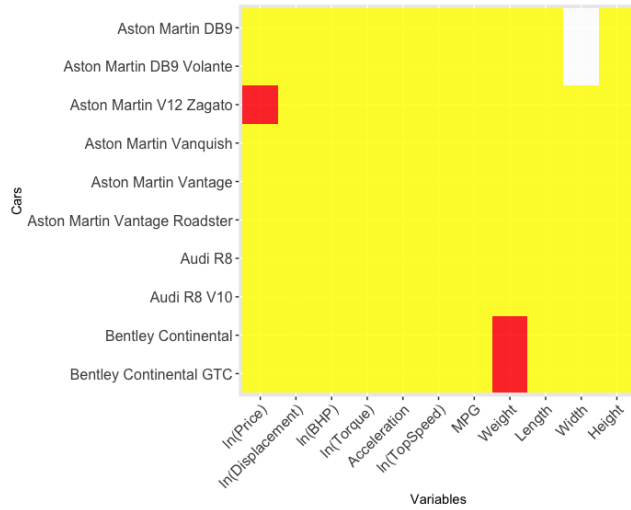
the other five variables, i.e., $\ln(\text{Displacement})$, $\ln(\text{BHP})$, $\ln(\text{Torque})$, Acceleration and $\ln(\text{TopSpeed})$, the percentage of reliable cells ranges from 94% to 99% and refers to both contaminated and missing values, except for $\ln(\text{Price})$ and Acceleration , which are fully observed. Considering separately the four variables mostly affected by unreliable cells, Figure 4 shows the standardized cellwise residuals, calculated as $(x_{ij} - \hat{x}_{ij(g)}) / \sqrt{\hat{C}_{ij(g)}}$, where $g = \arg \max_{g'=1, \dots, G} \hat{z}_{ig'}$. Missing data are not displayed in the plots, and the horizontal lines represent $\pm \sqrt{\chi_{1,0.99}^2}$. For instance, the Bentley Continental, Bentley Continental GCT,



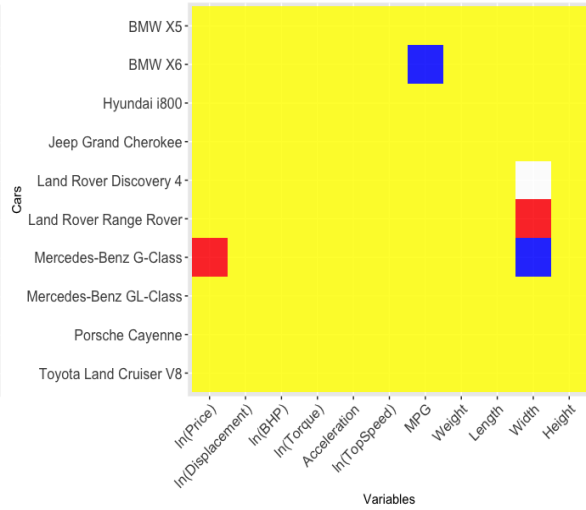
(a) Cluster 1



(b) Cluster 2



(c) Cluster 3



(d) Cluster 4

Figure 5: Top Gear data set: representation of cellwise outliers and their imputation for the ten representative cars per cluster. Yellow: reliable cells; blue: contaminated cells imputed with a higher value than the original one; red: contaminated cells imputed with a lower value than the original one; white: missing values

Bentley Mulsanne, Flying Spur, Rolls-Royce Phantom, Rolls-Royce Phantom Coupé, and Volkswagen Phaeton feature soundproofing materials and structural reinforcements that increase their weight, among other features (Figure 4a); the Aston Martin Cygnet, Smart fortwo, and Toyota iQ are shorter than typical city cars, whereas the SEAT Toledo, Honda Insight, and Proton GEN-2 are longer (Figure 4b). Other examples are the Land Rover Range Rover and Land Rover Range Rover Sport for Cluster 4, which have a width greater than expected for large SUVs or off-roaders (Figure 4c), while the Fiat Doblò and Subaru Forester have a height higher than that of crossovers (Figure 4d). It should be noted that for each variable, some cars may not be marginal outliers but could still be flagged as contaminated by cellGMM (black points in Figure 4) based on the cluster configuration, meaning they might actually be inlying points between components. Finally, an illustration of the unreliable cells for the most representative cars per cluster, as listed in Table 4, is shown in Figure 5. Here, it is notable that some cars, such as the Peugeot 107 in Cluster 2, display only one contaminated cell, whereas others have multiple, like the Lexus GS in Cluster 1, which has $\ln(\text{Torque})$ and $\ln(\text{Top Speed})$ significantly lower than expected for a mid-size sedan (Figure 5a), and the Mercedes-Benz G-Class that, although more expensive than typical off-roaders, has a lower width (Figure 5d).

5 Discussion

The cellGMM methodology introduced in this paper is designed to detect and handle contaminated cells in heterogeneous populations, as well as manage missing values. Following the new paradigm of cellwise contamination and the rationale of the EM, we have proposed

an algorithm that includes a concentration step to identify unreliable cells before the E- and M-steps, where the corresponding values are imputed and the Gaussian mixture model parameters are estimated, respectively. The estimation is constrained to ensure robustness and avoid degeneracies and spurious solutions. Compared to the existing methodology for model-based clustering in the presence of cellwise adulteration, cellGMM leverages the relationships among variables – especially when they are strong – by imputing the unreliable cells. In contrast, `sclust` trims, or more precisely, snips these cells from the parameter estimation.

While the proposal was initially illustrated by constraining the same proportion of contaminated cells per variable, a penalized version of cellGMM allows for automatic adjustments to avoid discarding valuable information and improve efficiency. The performance of these two approaches, in terms of clustering, parameter recovery, and data imputation, has been tested in a simulation study where cellGMM was compared to other robust and non-robust methodologies across both single and heterogeneous population frameworks. The examined scenarios cover simple and complex situations, considering different cluster configurations (well-separated and close components), data dimensionality (smaller and higher), outlier magnitude (less and more extreme), and information removal (missing data). Additionally, three real data applications illustrate the results of cellGMM in different fields and for various purposes, such as the classification of hyperspectral data, image reconstruction, and outlier detection in a data set where contaminated and missing values are not artificially generated.

Notwithstanding the results shown throughout the paper, several issues remain open for

future research as the proposal is one of the first attempts to handle cellwise outlier detection in mixture models. First and foremost, we will delve into a criterion for selecting the number of components, which is rather fixed in our experiments. Secondly, the procedure for the initialization of the cellGMM algorithm may be improved by performing a detailed study on the tuning parameter settings to balance performance and avoid trapping initial solutions in specific regions of the parameter space. Finally, the cellwise properties of the parameter estimators will be inspected.

Supplementary Materials

This text provides insights into the cellGMM algorithm (i.e., computations for the E- and M-step and initialization), as well as additional results from the simulation study and real data applications.

Software and data availability

The source code for cellGMM and an example code for the simulation study are available at <https://github.com/giorgiazaccaria/cellGMM>. The sources for the Carina Nebula and Top Gear data sets are reported in the paper, while the Homogenized Meat data set is available in the Supplemental Content of Murphy et al. (2010).

Acknowledgments

The research of Giorgia Zaccaria and Francesca Greselin was supported by Milano-Bicocca University Fund for Scientific Research, 2023-ATE-0448. The research of Luis A. García-Escudero, Agustín Mayo-Íscar and Francesca Greselin was partially supported by grant PID2021-128314NB-I00 funded by MCIN/AEI/ 10.13039/501100011033/FEDER. Francesca

Greselin’s research was also supported by PRIN2022 - 2022LANNKC.

Disclosure Statement

The authors have no conflicts of interest to declare.

References

- Alfons, A. (2021). robustHD: An R package for robust regression with high-dimensional data. *Journal of Open Source Software* 6(67), 3786.
- Alqallaf, F., S. Van Aelst, V. J. Yohai, and R. H. Zamar (2009). Propagation of outliers in multivariate data. *The Annals of Statistics* 37(1), 311–331.
- Cappozzo, A., F. Greselin, and T. B. Murphy (2021). Robust variable selection for model-based learning in presence of adulteration. *Computational Statistics & Data Analysis* 158, 107186.
- Cuesta-Albertos, J. A., A. Gordaliza, and C. Matran (1997). Trimmed k -means: An attempt to robustify quantizers. *The Annals of Statistics* 25(2), 553–576.
- Dempster, A. P., N. M. Laird, and D. B. Rubin (1977). Maximum likelihood from incomplete data via the EM algorithm. *Journal of the Royal Statistical Society, Series B (Statistical Methodology)* 39(1), 1–38.
- Downey, G. (1996). Authentication of food and food ingredients by near infrared spectroscopy. *Journal of Near Infrared Spectroscopy* 4(1), 47–61.
- Farcomeni, A. (2013). Snipping for robust k -means clustering under component-wise contamination. *Statistics and Computing* 24(6), 907–919.

- Farcomeni, A. (2014). Robust constrained clustering in presence of entry-wise outliers. *Technometrics* 56(1), 102–111.
- García-Escudero, L. A., A. Gordaliza, C. Matrán, and A. Mayo-Iscar (2008). A general trimming approach to robust cluster analysis. *The Annals of Statistics* 36(3), 1324–1345.
- García-Escudero, L. A., A. Gordaliza, and A. Mayo-Iscar (2014). A constrained robust proposal for mixture modeling avoiding spurious solutions. *Advances in Data Analysis and Classification* 8(1), 27–43.
- García-Escudero, L. A., D. Rivera-García, A. Mayo-Iscar, and J. Ortega (2021). Cluster analysis with cellwise trimming and applications for the robust clustering of curves. *Information Sciences* 573, 100–124.
- Huber, P. J. (1964). Robust estimation of a location parameter. *The Annals of Mathematical Statistics* 35(1), 73–101.
- Hubert, M., P. J. Rousseeuw, and W. V. den Bossche (2019). MacroPCA: An all-in-one PCA method allowing for missing values as well as cellwise and rowwise outliers. *Technometrics* 61(4), 459–473.
- Little, R. J. A. and D. B. Rubin (2019). *Statistical Analysis with Missing Data* (3 ed.). John Wiley & Sons, Hoboken.
- Maitra, R. and V. Melnykov (2010). Simulating data to study performance of finite mixture modeling and clustering algorithms. *Journal of Computational and Graphical Statistics* 19(2), 354–376.

- McElhinney, J., G. Downey, and T. Fearn (1999). Chemometric processing of visible and near infrared reflectance spectra for species identification in selected raw homogenised meats. *Journal of Near Infrared Spectroscopy* 7(3), 145–154.
- McLachlan, G. J. and T. Krishnan (2008). *The EM algorithm and extensions* (2 ed.). Wiley, Hoboken.
- McLachlan, G. J. and D. Peel (2000). *Finite mixture models*. Wiley, New York.
- Murphy, T. B., N. Dean, and A. E. Raftery (2010). Variable selection and updating in model-based discriminant analysis for high dimensional data with food authenticity applications. *The Annals of Applied Statistics* 4(1), 396–421.
- Neykov, N. M., P. Filzmoser, R. Dimova, and P. N. Neytchev (2007). Robust fitting of mixtures using the trimmed likelihood estimator. *Computational Statistics & Data Analysis* 52(1), 299–308.
- Punzo, A. and P. D. McNicholas (2016). Parsimonious mixtures of multivariate contaminated normal distributions. *Biometrical Journal* 58(6), 1506–1537.
- Raymaekers, J. and P. J. Rousseeuw (2021). Handling cellwise outliers by sparse regression and robust covariance. *Journal of Data Science, Statistics, and Visualisation* 1(3), <https://doi.org/10.52933/jdssv.v1i3.18>.
- Raymaekers, J. and P. J. Rousseeuw (2023). The cellwise minimum covariance determinant estimator. *Journal of the American Statistical Association*, 1–12, <https://doi.org/10.1080/01621459.2023.2267777>.

- Raymaekers, J. and P. J. Rousseeuw (2024). Challenges of cellwise outliers. *Econometrics and Statistics*, <https://doi.org/10.1016/j.ecosta.2024.02.002>.
- Rousseeuw, P. J. (1984). Least median of squares regression. *Journal of the American Statistical Association* 79(388), 871–880.
- Rousseeuw, P. J. (1985). Multivariate estimation with high breakdown point. In W. Grossmann, G. Pflug, I. Vincze, and W. Wertz (Eds.), *Mathematical Statistics and Applications*, pp. 283–297.
- Rousseeuw, P. J. and K. van Driessen (1999). A fast algorithm for the minimum covariance determinant estimator. *Technometrics* 41(3), 212–223.
- Rubin, D. B. (1976). Inference and missing data. *Biometrika* 63(3), 581–592.
- Tong, H. and C. Tortora (2022). Model-based clustering and outlier detection with missing data. *Advances in Data Analysis and Classification* 16(1), 5–30.
- Wang, H., Q. Zhang, B. Luo, and S. Wei (2004). Robust mixture modelling using multivariate t-distribution with missing information. *Pattern Recognition Letters* 25(6), 701–710.
- Yao, W. (2015). Label switching and its solutions for frequentist mixture models. *Journal of Statistical Computation and Simulation* 85(5), 1000–1012.
- Zhang, M., Y. Song, and W. Dai (2024). Fast robust location and scatter estimation: A depth-based method. *Technometrics* 66(1), 14–27.

Supplementary Material to “Cellwise outlier detection in heterogeneous populations”

Giorgia Zaccaria

Department of Statistics and Quantitative Methods, University of Milano-Bicocca
and

Luis A. García-Escudero

Department of Statistics and Operational Research, University of Valladolid
and

Francesca Greselin

Department of Statistics and Quantitative Methods, University of Milano-Bicocca
and

Agustín Mayo-Íscar

Department of Statistics and Operational Research, University of Valladolid

September 13, 2024

1 The cellGMM algorithm

1.1 Computations for the E- and M-step

In this section, we illustrate the computations required in the E- and M-step of the cell-GMM algorithm. In the E-step, we compute the expected values $\mathbb{E}[Z_{ig} | \mathbf{x}_{i[\mathbf{w}_i^{(t+1)}]}; \widehat{\Psi}^{(t)}]$, $\mathbb{E}[\mathbf{X}_{i[\mathbf{w}_i^{(t+1)c}]} | \mathbf{x}_{i[\mathbf{w}_i^{(t+1)}]}, z_{ig} = 1; \widehat{\Psi}^{(t)}]$ and $\mathbb{E}[(\mathbf{X}_{i[\mathbf{w}_i^{(t+1)c}]} - \boldsymbol{\mu}_{g[\mathbf{w}_i^{(t+1)c}]})(\mathbf{X}_{i[\mathbf{w}_i^{(t+1)c}]} - \boldsymbol{\mu}_{g[\mathbf{w}_i^{(t+1)c}]})' | \mathbf{x}_{i[\mathbf{w}_i^{(t+1)}]}, z_{ig} = 1; \widehat{\Psi}^{(t)}]$, which can be easily derived following Ghahramani and Jordan (1994):

$$\mathbb{E}[Z_{ig} | \mathbf{x}_{i[\mathbf{w}_i^{(t+1)}]}; \widehat{\Psi}^{(t)}] = \frac{\widehat{\pi}_g^{(t)} \phi_{p[\mathbf{w}_i^{(t+1)}]}(\mathbf{x}_{i[\mathbf{w}_i^{(t+1)}]}; \widehat{\boldsymbol{\mu}}_{g[\mathbf{w}_i^{(t+1)}]}^{(t)}, \widehat{\boldsymbol{\Sigma}}_{g[\mathbf{w}_i^{(t+1)}, \mathbf{w}_i^{(t+1)}]}^{(t)})}{\sum_{h=1}^G \widehat{\pi}_h^{(t)} \phi_{p[\mathbf{w}_i^{(t+1)}]}(\mathbf{x}_{i[\mathbf{w}_i^{(t+1)}]}; \widehat{\boldsymbol{\mu}}_{h[\mathbf{w}_i^{(t+1)}]}^{(t)}, \widehat{\boldsymbol{\Sigma}}_{h[\mathbf{w}_i^{(t+1)}, \mathbf{w}_i^{(t+1)}]}^{(t)})} := z_{ig}^{(t+1)} \quad (1)$$

$$\mathbb{E}[\mathbf{X}_{i[\mathbf{w}_i^{(t+1)}c_1]} | \mathbf{x}_{i[\mathbf{w}_i^{(t+1)}]}, z_{ig} = 1; \widehat{\Psi}^{(t)}] = \widehat{\boldsymbol{\mu}}_{g[\mathbf{w}_i^{(t+1)}c_1]}^{(t)} + \widehat{\boldsymbol{\Sigma}}_{g[\mathbf{w}_i^{(t+1)}c, \mathbf{w}_i^{(t+1)}]}^{(t)} \left(\widehat{\boldsymbol{\Sigma}}_{g[\mathbf{w}_i^{(t+1)}, \mathbf{w}_i^{(t+1)}]}^{(t)} \right)^{-1} (\mathbf{x}_{i[\mathbf{w}_i^{(t+1)}]} - \widehat{\boldsymbol{\mu}}_{g[\mathbf{w}_i^{(t+1)}]}^{(t)}) := \widehat{\mathbf{x}}_{i[\mathbf{w}_i^{(t+1)}c_1]^{(g)}}^{(t+1)} \quad (2)$$

$$\mathbb{E}[(\mathbf{X}_{i[\mathbf{w}_i^{(t+1)}c_1]} - \boldsymbol{\mu}_{g[\mathbf{w}_i^{(t+1)}c_1]})(\mathbf{X}_{i[\mathbf{w}_i^{(t+1)}c_1]} - \boldsymbol{\mu}_{g[\mathbf{w}_i^{(t+1)}c_1]})' | \mathbf{x}_{i[\mathbf{w}_i^{(t+1)}]}, z_{ig} = 1; \widehat{\Psi}^{(t)}] = \widetilde{\mathbf{C}}_{i(g)}^{(t+1)} + \widetilde{\mathbf{C}}_{i(g)}^{(t+1)}, \quad (3)$$

where $\widetilde{\mathbf{C}}_{i(g)}^{(t+1)} := \widehat{\boldsymbol{\Sigma}}_{g[\mathbf{w}_i^{(t+1)}c, \mathbf{w}_i^{(t+1)}c_1]}^{(t)} - \widehat{\boldsymbol{\Sigma}}_{g[\mathbf{w}_i^{(t+1)}c, \mathbf{w}_i^{(t+1)}]}^{(t)} \left(\widehat{\boldsymbol{\Sigma}}_{g[\mathbf{w}_i^{(t+1)}, \mathbf{w}_i^{(t+1)}]}^{(t)} \right)^{-1} \widehat{\boldsymbol{\Sigma}}_{g[\mathbf{w}_i^{(t+1)}, \mathbf{w}_i^{(t+1)}c_1]}^{(t)}$ and $\widetilde{\mathbf{C}}_{i(g)}^{(t+1)} = \left(\widehat{\mathbf{x}}_{i[\mathbf{w}_i^{(t+1)}c_1]^{(g)}}^{(t+1)} - \widehat{\boldsymbol{\mu}}_{g[\mathbf{w}_i^{(t+1)}c_1]}^{(t)} \right) \left(\widehat{\mathbf{x}}_{i[\mathbf{w}_i^{(t+1)}c_1]^{(g)}}^{(t+1)} - \widehat{\boldsymbol{\mu}}_{g[\mathbf{w}_i^{(t+1)}c_1]}^{(t)} \right)'$.

The M-step provides the parameter estimates by considering the *completed* data $\left\{ \left\{ \widetilde{\mathbf{x}}_{i(g)}^{(t+1)} = (\mathbf{x}_{i[\mathbf{w}_i^{(t+1)}]}, \widehat{\mathbf{x}}_{i[\mathbf{w}_i^{(t+1)}c_1]^{(g)}}^{(t+1)}) \right\}_{g=1}^G \right\}_{i=1}^n$.

Update of $\boldsymbol{\pi}$. The weights $\boldsymbol{\pi} = \{\pi_g\}_{g=1}^G$ are updated as

$$\widehat{\pi}_g^{(t+1)} = \frac{\sum_{i=1}^n z_{ig}^{(t+1)}}{n}. \quad (4)$$

Update of $\boldsymbol{\theta}$. The component mean vectors and covariance matrices in $\boldsymbol{\theta} = \{\boldsymbol{\mu}_g, \boldsymbol{\Sigma}_g\}_{g=1}^G$ are updated as

$$\widehat{\boldsymbol{\mu}}_g^{(t+1)} = \frac{\sum_{i=1}^n z_{ig}^{(t+1)} \widetilde{\mathbf{x}}_{i(g)}^{(t+1)}}{\sum_{i=1}^n z_{ig}^{(t+1)}}, \quad (5)$$

$$\widehat{\boldsymbol{\Sigma}}_g^{(t+1)} = \frac{\sum_{i=1}^n z_{ig}^{(t+1)} \left[(\widetilde{\mathbf{x}}_{i(g)}^{(t+1)} - \widehat{\boldsymbol{\mu}}_g^{(t+1)}) (\widetilde{\mathbf{x}}_{i(g)}^{(t+1)} - \widehat{\boldsymbol{\mu}}_g^{(t+1)})' + \widetilde{\mathbf{C}}_{i(g)}^{(t+1)} \right]}{\sum_{i=1}^n z_{ig}^{(t+1)}}. \quad (6)$$

1.2 Initialization

The procedure proposed for the initialization of the cellGMM algorithm is detailed below.

This is entirely based on several applications of the TCLUST method, which is implemented via the R package `tclust` (Fritz et al., 2012).

Step 1 Initialization of \mathbf{W} : the initial solution for \mathbf{W} is obtained by applying TCLUST individually to each variable and to pairs of variables with a fixed α_{tclust} trimming level. The estimated parameters per component from these TCLUST applications are used to compute the Mahalanobis distances. Roughly speaking, the smallest Mahalanobis distance across components for each unit is considered in both univariate and bivariate TCLUST applications. Proportions α_1 and α_2 of cells per variable are flagged as outliers based on the distribution of the Mahalanobis distances computed via univariate and bivariate TCLUST, respectively. Unreliable cells per variable previously identified through univariate TCLUST are excluded from the bivariate TCLUST outlier detection. A more detailed pseudo-code description of this procedure is provided in Algorithm 1. Notice that in the pseudo-code we refer to the Mahalanobis distances as MD.

Step 2 Initialization of Ψ :

2.1 n_{rep} subsets of q out of p variables are randomly selected. For each reduced set of q variables, TCLUST is implemented with a fixed trimming level α_{A_1} on the resulting completely reliable observations to obtain G component mean vectors and covariance matrices. It is worth noting that reducing the set of variables

considered increases the number of completely reliable observations as input for TCLUS_T, where the reliability of an observation is based upon the initial configuration of \mathbf{W} (see Step 1). The two sets composed of n_{rep} parameters each resulting from TCLUS_T are stored into $\mathbf{tclust}_{\boldsymbol{\mu}}$ (n_{rep} location vectors) and $\mathbf{tclust}_{\boldsymbol{\Sigma}}$ (n_{rep} scatter matrices), respectively.

2.2 In this part, a version of trimmed k -means (Cuesta-Albertos et al., 1997) accommodated for the presence of missing values is implemented to obtain a partition of the n_{rep} elements in $\mathbf{tclust}_{\boldsymbol{\mu}}$ into G groups. The corresponding “centers of centers” are then used to initialize $\{\boldsymbol{\mu}_g\}_{g=1}^G$. Specifically, according to a multi-start procedure, a matrix \mathbf{N} representing G centers of center groups is initialized by one of the n_{rep} elements in $\mathbf{tclust}_{\boldsymbol{\mu}}$. Then, \mathbf{N} is iteratively updated across n_{iter} iterations by assigning the n_{rep} elements in $\mathbf{tclust}_{\boldsymbol{\mu}}$ to the nearest center of centers in \mathbf{N} and recomputing \mathbf{N} accordingly. The latter is obtained as the mean of centers in $\mathbf{tclust}_{\boldsymbol{\mu}}$ per group, after having discarded a proportion α_{A2} of them according to their squared Euclidean distances. Among several random starts (n_{start}), the selected solution for $\{\boldsymbol{\mu}_g\}_{g=1}^G$ is \mathbf{N} that minimizes the total squared Euclidean distances between the centers in $\mathbf{tclust}_{\boldsymbol{\mu}}$ and the centers of center groups in \mathbf{N} . The resulting partition in groups is also used for computing the G component covariance matrices $\{\boldsymbol{\Sigma}_g\}_{g=1}^G$ as the means of the elements in $\mathbf{tclust}_{\boldsymbol{\Sigma}}$ per group. It is worth noting that this procedure does not necessarily guarantee the positive definiteness of $\boldsymbol{\Sigma}_g$, as the mean of covariance matrices in $\mathbf{tclust}_{\boldsymbol{\Sigma}}$ refers to different subsets of variables. Therefore, we impose on $\{\boldsymbol{\Sigma}_g\}_{g=1}^G$ the

eigenvalue-ratio constraint reported in (4) of the paper, which entails obtaining positive definite matrices. This constraint is implemented throughout the cellGMM algorithm via the efficient procedure reported in Fritz et al. (2013). The weights $\boldsymbol{\pi} = \{\pi_g\}_{g=1}^G$ are figured up after assigning each observation to a component by considering the minimum squared Euclidean distance from $\{\boldsymbol{\mu}_g\}_{g=1}^G$. A more detailed pseudo-code description of the procedure proposed in this Step 2.2 is illustrated in Algorithm 2.

The initialization described herein depends on several tuning parameters. In our experiments, we set those regarding the trimming levels according to the true level of contamination, denoted as α_{true} . Specifically, we set $\alpha_{\text{tclust}} = 2 \cdot \alpha_{\text{true}}$, $\alpha_1 = \alpha_2 = \alpha_{\text{true}}$, $\alpha_{A1} = \alpha_{\text{true}}$ and $\alpha_{A2} = 2 \cdot \alpha_{\text{true}}$. If α_{true} is unknown, as it is usually the case in real-world applications, we suggest considering a conservative level of contamination as the true value, e.g., 0.03 or 0.05 (i.e., assuming 3% or 5% of contamination). The tuning parameter q , which controls the number of variables selected in the first step of the initialization of $\boldsymbol{\Psi}$, is fixed to $\lfloor \frac{p}{2} \rfloor + 1$. This choice guarantees that the subsets of sampled variables overlap for at least one variable. The remaining parameters for the initialization of $\boldsymbol{\Psi}$ are set as follows: $n_{\text{rep}} = 40$, $n_{\text{start}} = 10$ and $n_{\text{iter}} = 10$. This configuration of the tuning parameters proves to be effective in our experiments. However, their setting could be improved by performing a specific simulation study on the initialization, which is out of the scope of this paper primarily focused on the main part of the cellGMM algorithm.

Algorithm 1 Initialization of \mathbf{W} (Step 1)

1: **Input:** \mathbf{X} , α_{tclust} , α_1 , α_2 , G

2: $p \leftarrow$ number of columns (variables) in \mathbf{X}

Univariate TCLUS

3: **for** $j_1 \leftarrow 1 : p$ **do**

4: $\mathbf{tc}_1[[j_1]] \leftarrow \text{tclust}(\mathbf{X}[,j_1], \mathbf{k} = G, \text{alpha} = \alpha_{\text{tclust}})$, where only observed units in variable j_1 are considered

5: **end for**

6: **for** $j_1 \leftarrow 1 : p$ **do**

7: $\text{MD}_1 \leftarrow$ compute MD for each unit per component according to the parameters obtained from univariate TCLUS

8: $\mathbf{f}_1[j_1] \leftarrow$ select the minimum MD_1 across components

9: **end for**

Detection of cellwise outliers through univariate TCLUS

10: $\text{qq}_1 \leftarrow \text{quantile}(\mathbf{f}_1, 1 - \alpha_1, \text{na.rm} = \text{TRUE})$

11: $\mathbf{W}_{(1)}[\mathbf{f}_1 > \text{qq}_1] \leftarrow 0$, where $\mathbf{W}_{(1)}$ has been initialized as $\mathbf{1}_n \mathbf{1}'_p$ (i.e., an $n \times p$ matrix of ones)

Bivariate TCLUS

12: **for** $j_1 \leftarrow 1 : (p - 1)$ **do**

13: **for** $j_2 \leftarrow (j_1 + 1) : p$ **do**

14: $\mathbf{tc}_2[[j_1]][[j_2]] \leftarrow \text{tclust}(\text{cbind}(\mathbf{X}[,j_1], \mathbf{X}[,j_2]), \mathbf{k} = G, \text{alpha} = \alpha_{\text{tclust}})$, where only observed units in both variables j_1 and j_2 are considered

```

15:   end for
16: end for
17: for  $j_1 \leftarrow 1 : (p - 1)$  do
18:   for  $j_2 \leftarrow (j_1 + 1) : p$  do
19:      $MD_2 \leftarrow$  compute MD for each unit per component according to the parameters
        from bivariate TCLUS
20:      $f_2[, j_1, j_2] \leftarrow$  select the minimum  $MD_2$  across components
21:   end for
22: end for

```

Detection of cellwise outliers through bivariate TCLUS by excluding the
already flagged cells

```

23: for  $j \leftarrow 1 : p$  do
24:    $f_2[\mathbf{W}_{(1)}[, j] == 0, j, ] \leftarrow$  NA
25:    $f_2[\mathbf{W}_{(1)}[, j] == 0, , j] \leftarrow$  NA
26: end for
27: for  $j \leftarrow 1 : p$  do
28:    $ff_2[, j] \leftarrow$  apply( $f_2[, j, ], 1, \text{sum}, \text{na.rm} = \text{TRUE}$ ) + apply( $f_2[, , j], 1, \text{sum}, \text{na.rm} =$ 
        TRUE)
29: end for
30:  $ff_2[\mathbf{W}_{(1)} == 0] \leftarrow$  NA
31:  $qq_2 \leftarrow$  quantile( $ff_2, 1 - \frac{\alpha_1}{1 - \alpha_2}, \text{na.rm} = \text{TRUE}$ )

```

-
- 32: $\mathbf{W}_{(2)}[\mathbf{f}\mathbf{f}_2 > \mathbf{q}\mathbf{q}_2] \leftarrow 0$, where $\mathbf{W}_{(2)}$ has been initialized as $\mathbf{1}_n\mathbf{1}'_p$ and NA values in $\mathbf{W}_{(2)}$ are replaced by 1
- 33: $\mathbf{W} \leftarrow \mathbf{W}_{(1)} \odot \mathbf{W}_{(2)}$ (Hadamard or element-wise product), where cells corresponding to NA values in \mathbf{X} are set to 0
- 34: **Output:** \mathbf{W}
-

2 Simulation study: additional results

We present herein the results of a simulation study on six additional scenarios beyond those reported in Section 3 of the paper. These are divided in three scenarios with less extreme cellwise outliers and missing data (Section 2.1) and three scenarios with more extreme contamination (Section 2.2). In addition to the indices already introduced in Section 3 of the paper for assessing the models' performance, we report the Adjusted Rand Index (ARI, Hubert and Arabie, 1985), the Root Mean Squared Error of the posterior probabilities and the Mean Squared Error of the prior probabilities. These indices for Scenarios 1-3 are reported in Table 1.

2.1 Less extreme outliers

The three additional scenarios with less extreme outliers are as follows: *Scenario 4* and *Scenario 5* with $n = 200, p = 5, G = 2$, non-spherical with $\mathbf{\Sigma}_1 = [\sigma_{ii} = 1, \sigma_{ij} = 0.9^{|i-j|}, i, j = 1, \dots, p, i \neq j]$ and $\mathbf{\Sigma}_2$ obtained by an orthogonal rotation of $\mathbf{\Sigma}_1$, unbalanced ($\boldsymbol{\pi} = [0.3, 0.7]$) and well-separated and close components, respectively; *Scenario 6* with $n = 400, p = 15, G = 4$, non-spherical with $\mathbf{\Sigma}_1 = \mathbf{\Sigma}_2 = [\sigma_{ii} = 1, \sigma_{ij} = 0.9^{|i-j|}, i, j = 1, \dots, p, i \neq j]$ and

Algorithm 2 Step 2.2 of the initialization of Ψ

- 1: **Input:** $\mathbf{X}, G, \alpha_{A2}, n_{\text{start}}, n_{\text{iter}}, \text{tclust}_{\mu}, \text{tclust}_{\Sigma}$ ($n_{\text{iter}}, \text{tclust}_{\mu}$ and tclust_{Σ} come from Step 2.1)
 - 2: $\text{obj.best} \leftarrow +\infty$
 - 3: **for** $\text{start} \leftarrow 1 : n_{\text{start}}$ **do**
 - 4: Sample one of the n_{rep} subsets of variables used for obtaining tclust_{μ} and tclust_{Σ} and initialize the centers of center groups in \mathbf{N} as the tclust_{μ} corresponding to the selected repetition
 - 5: **for** $\text{iter} \leftarrow 1 : n_{\text{iter}}$ **do**
 - 6: Compute distances between the centers tclust_{μ} and the centers of center groups in \mathbf{N}
 - 7: Assign each center in tclust_{μ} to the corresponding group $g \in \{1, \dots, G\}$ according to the minimum distance
 - 8: Update the rows of \mathbf{N} as the mean of the corresponding centers in tclust_{μ} assigned to the g th group, $g = 1, \dots, G$, by excluding a proportion α_{A2} of centers in tclust_{μ} with the most “extreme” distances
 - 9: **end for**
 - 10: $\text{obj} \leftarrow$ sum of distances across n_{rep} repetitions and G groups
 - 11: **if** $\text{obj} < \text{obj.best}$ **then**
 - 12: Update $\{\boldsymbol{\mu}_g\}_{g=1}^G$ and group assignment of the centers in tclust_{μ}
 - 13: $\text{obj.best} \leftarrow \text{obj}$
 - 14: **end if**
 - 15: **end for**
-

-
- 16: Compute $\{\Sigma_g\}_{g=1}^G$ as the mean of the covariance matrices in `tclust Σ` according to the group assignment obtained for the centers in `tclust μ` and check for the eigenvalue-ratio constraint
 - 17: Compute the weights $\{\pi_g\}_{g=1}^G$ according to the minimum squared Euclidean distance of each observation from $\{\mu_g\}_{g=1}^G$
 - 18: **Output:** initial parameters $\Psi = \{\pi, \theta\}$, where $\pi = \{\pi_g\}_{g=1}^G$ and $\theta = \{\mu_g, \Sigma_g\}_{g=1}^G$
-

$\Sigma_3 = \Sigma_4$ obtained by an orthogonal rotation of Σ_1 , unbalanced ($\pi = [0.2, 0.2, 0.3, 0.3]$) and well-separated components. For each scenario, we generate 100 data matrices that we contaminate with 0%, 5% and 10% of outliers randomly drawn from a uniform distribution in the interval $[-10, 10]$, ensuring they do not lie within the 99th percentile ellipsoid of any component. Moreover, we randomly remove 5% of the cells which have not been contaminated to obtain samples with missing data. Due to the latter, the only models we can compare to cellGMM are those included in the R package `MixtureMissing`, i.e., MNM, MCNM, M t M, since they can handle missing values.

The results of the classification performance and parameter estimates are reported in Tables 2 and 3. As the level of contamination and the dimensionality of the data increase, the difference between cellGMM, specifically its penalized version (i.e. `cellGMM.penb`), and the competitors grows. Notably, in Scenario 6 with 10% of cellwise outliers, `cellGMM.penb` improves the parameter estimates compared to `cellGMM.pen0`, although this improvement is not reflected in the averaged ARI over the 100 samples. This is due to the distribution of the contaminated data being, by chance, well balanced among variables. In Table 4, we illustrate the results of the model on outlier detection and the corresponding value

Table 1: Number of samples on which each model can be properly computed (# samp.), mean of the Adjusted Rand Index (mARI), Root Mean Squared Error of the posterior probabilities (RMSE_z) and Mean Squared Error (MSE_π) of the prior probabilities per scenario, percentage of contamination, and model

% out.	Model	Scenario 1				Scenario 2				Scenario 3			
		# samp.	mARI	RMSE _z	MSE _π	# samp.	mARI	RMSE _z	MSE _π	# samp.	mARI	RMSE _z	MSE _π
0	cellGMM.pen0	100	0.91	0.13	0.00	100	0.58	0.30	0.00	100	1.00	0.01	0.00
	cellGMM.penb	100	1.00	0.00	0.00	100	0.78	0.17	0.00	100	1.00	0.00	0.00
	TCLUST	100	1.00	0.00	0.00	100	0.80	0.15	0.00	100	1.00	0.00	0.00
	schust_25	98	0.87	0.02	0.02	100	0.33	0.36	0.01	0			
	MNM	100	1.00	0.00	0.00	100	0.83	0.10	0.01	100	1.00	0.00	0.00
	MCNM	100	1.00	0.00	0.00	100	0.83	0.11	0.01	100	1.00	0.00	0.00
	MtM	100	1.00	0.00	0.00	100	0.84	0.10	0.01	100	1.00	0.00	0.00
5	cellGMM.pen0	100	0.88	0.16	0.00	100	0.43	0.38	0.01	100	0.99	0.02	0.00
	cellGMM.penb	100	0.94	0.10	0.00	100	0.62	0.27	0.01	100	0.99	0.02	0.00
	TCLUST	100	0.74	0.26	0.00	100	0.59	0.31	0.00	100	0.24	0.51	0.01
	schust_25	97	0.81	0.16	0.04	94	0.25	0.42	0.02	0			
	schust_5	93	0.93	0.13	0.06	90	0.41	0.33	0.02	90	0.94	0.12	0.10
	MNM	100	0.64	0.31	0.01	100	0.00	0.60	0.02	100	0.89	0.13	0.00
	MCNM	100	0.69	0.27	0.00	100	0.02	0.58	0.03	100	0.81	0.23	0.00
MtM	100	0.71	0.26	0.00	100	0.03	0.57	0.03	100	0.72	0.31	0.00	
10	cellGMM.pen0	100	0.82	0.19	0.00	100	0.42	0.38	0.01	100	0.94	0.10	0.00
	cellGMM.penb	100	0.86	0.16	0.00	100	0.52	0.31	0.01	100	0.95	0.08	0.00
	TCLUST	100	0.33	0.46	0.01	100	0.00	0.66	0.12	100	0.07	0.56	0.01
	schust_25	93	0.75	0.22	0.05	88	0.27	0.42	0.02	0			
	schust_10	88	0.87	0.17	0.06	63	0.34	0.38	0.03	53	0.77	0.25	0.12
	MNM	100	0.41	0.42	0.04	100	0.00	0.69	0.08	100	0.69	0.25	0.00
	MCNM	100	0.56	0.34	0.01	100	0.00	0.62	0.02	100	0.50	0.34	0.01
MtM	100	0.55	0.34	0.01	100	0.00	0.61	0.02	100	0.41	0.39	0.01	

Table 2: Number of samples on which each model can be properly computed (# samp.), mean of the Adjusted Rand Index and Misclassification Rate (mARI and mMR), Root Mean Squared Error of the posterior probabilities (RMSE_z), Mean Squared Error (MSE) of the prior probabilities and component mean vectors, and Kullback-Leibler (KL) discrepancy for the component covariance matrices per scenario, percentage of contamination, and model

		Scenario 4								
% out.	Method	# samp.	mARI	mMR	RMSE _z	MSE _π	MSE _{μ₁}	MSE _{μ₂}	KL _{Σ₁}	KL _{Σ₂}
0	cellGMM.pen0	100	0.95	0.01	0.10	0.00	0.02	0.01	1.95	1.65
	cellGMM.penb	100	1.00	0.00	0.00	0.00	0.02	0.01	0.41	0.22
	MNM	100	1.00	0.00	0.00	0.00	0.02	0.01	0.29	0.12
	MCNM	80	1.00	0.00	0.00	0.00	0.02	0.01	0.31	0.15
	MtM	100	1.00	0.00	0.00	0.00	0.02	0.01	0.30	0.12
5	cellGMM.pen0	100	0.87	0.03	0.17	0.00	0.06	0.01	2.19	1.06
	cellGMM.penb	100	0.95	0.01	0.10	0.00	0.02	0.01	0.66	0.25
	MNM	100	0.69	0.09	0.29	0.01	0.51	0.03	158.99	35.45
	MCNM	16	0.71	0.08	0.26	0.01	0.02	0.01	0.98	0.24
	MtM	100	0.67	0.09	0.28	0.01	0.03	0.01	2.23	0.40
10	cellGMM.pen0	100	0.91	0.02	0.13	0.00	0.03	0.01	1.25	1.87
	cellGMM.penb	100	0.92	0.02	0.11	0.00	0.02	0.01	0.54	2.27
	MNM	100	0.46	0.16	0.40	0.03	1.01	0.08	274.22	73.96
	MCNM	31	0.55	0.13	0.34	0.02	0.03	0.02	4.04	1.98
	MtM	100	0.56	0.13	0.33	0.01	0.05	0.02	14.57	2.53
		Scenario 5								
% out.	Method	# samp.	mARI	mMR	RMSE _z	MSE _π	MSE _{μ₁}	MSE _{μ₂}	KL _{Σ₁}	KL _{Σ₂}
0	cellGMM.pen0	100	0.85	0.04	0.18	0.00	0.05	0.01	2.00	1.74
	cellGMM.penb	100	0.96	0.01	0.08	0.00	0.02	0.01	0.46	0.22
	MNM	100	0.99	0.00	0.03	0.00	0.02	0.01	0.29	0.12
	MCNM	78	0.99	0.00	0.03	0.00	0.02	0.01	0.33	0.14
	MtM	100	0.99	0.00	0.03	0.00	0.02	0.01	0.30	0.12
5	cellGMM.pen0	100	0.79	0.05	0.21	0.00	0.09	0.01	2.25	1.22
	cellGMM.penb	100	0.89	0.03	0.14	0.00	0.04	0.01	1.25	0.47
	MNM	100	0.50	0.15	0.38	0.02	0.32	0.03	170.24	13.94
	MCNM	24	0.61	0.11	0.31	0.01	0.03	0.01	4.73	0.29
	MtM	100	0.59	0.12	0.33	0.01	0.03	0.01	3.31	0.48
10	cellGMM.pen0	100	0.75	0.06	0.21	0.00	0.07	0.01	1.52	0.71
	cellGMM.penb	100	0.76	0.06	0.19	0.00	0.05	0.01	0.84	0.28
	MNM	100	0.05	0.45	0.65	0.07	0.96	0.57	153.65	244.85
	MCNM	25	0.32	0.23	0.43	0.02	0.18	0.05	28.99	16.59
	MtM	100	0.33	0.22	0.43	0.01	0.11	0.03	54.27	10.47

imputation for the aforementioned models, as well as cellMCD and DI. It should be noted that, unlike for Scenarios 1-3 analyzed in the paper, Table 4 shows non-null values of indices for the imputation evaluation of the model-based clustering competitors, referring only to the missing values. Null values indicate cases where the models cannot be run on any sample because errors occur in the code. Overall, cellGMM.penb outperforms the competitors by balancing good performance on TP% and FP% and data imputation.

Table 3: Number of samples on which each model can be properly computed (# samp.), mean of the Adjusted Rand Index and Misclassification Rate (mARI and mMR), Root Mean Squared Error of the posterior probabilities (RMSE_z), Mean Squared Error (MSE) of the prior probabilities and component mean vectors, and Kullback-Leibler (KL) discrepancy for the component covariance matrices per scenario, percentage of contamination, and model

		Scenario 6												
% out.	Method	# samp.	mARI	mMR	RMSE _z	MSE _π	MSE _{μ₁}	MSE _{μ₂}	MSE _{μ₃}	MSE _{μ₄}	KL _{Σ₁}	KL _{Σ₂}	KL _{Σ₃}	KL _{Σ₄}
0	cellGMM.pen0	100	1.00	0.00	0.00	0.00	0.01	0.02	0.01	0.01	8.71	8.81	8.72	8.63
	cellGMM.penb	100	1.00	0.00	0.00	0.00	0.01	0.01	0.01	0.01	2.58	2.58	2.12	2.15
	MNM	100	1.00	0.00	0.00	0.00	0.01	0.01	0.01	0.01	1.86	1.88	1.17	1.20
	MCNM	13	1.00	0.00	0.00	0.00	0.01	0.01	0.01	0.01	1.92	1.97	1.15	1.20
	MtM	100	1.00	0.00	0.00	0.00	0.01	0.01	0.01	0.01	1.86	1.89	1.17	1.20
5	cellGMM.pen0	100	0.91	0.05	0.03	0.00	0.02	1.21	0.06	0.29	16.31	59.41	21.59	39.87
	cellGMM.penb	100	0.95	0.03	0.02	0.00	0.01	0.74	0.08	0.27	2.58	44.64	11.75	21.62
	MNM	100	0.76	0.10	0.18	0.00	0.52	0.52	0.26	0.47	328.50	471.12	443.58	571.69
	MCNM	0												
	MtM	100	0.77	0.09	0.26	0.00	0.04	0.04	0.02	0.02	58.41	47.42	21.38	26.80
10	cellGMM.pen0	100	0.99	0.01	0.03	0.00	0.10	0.02	0.01	0.01	7.50	7.02	6.25	5.78
	cellGMM.penb	99	0.98	0.01	0.04	0.00	0.15	0.03	0.01	0.01	5.56	5.65	3.80	3.15
	MNM	100	0.57	0.21	0.22	0.00	0.95	1.40	0.84	1.37	636.71	906.19	810.46	1050.18
	MCNM	0												
	MtM	99	0.44	0.28	0.40	0.02	1.50	1.25	0.26	0.52	399.12	373.27	256.55	433.39

Table 4: Statistics on outlier detection and imputation: percentage of True Positive and False Positive (%TP and %FP), Mean Absolute Error (MAE) and Root Mean Squared Error (RMSE) in comparing the original and imputed data matrices per scenario, percentage of contamination, and model

		Scenario 4				Scenario 5				Scenario 6			
% out.	Method	%TP	%FP	MAE	RMSE	%TP	%FP	MAE	RMSE	%TP	%FP	MAE	RMSE
0	cellGMM,pen0	19.63	0.24	0.65		19.67	0.24	0.60		20.00	0.19	0.45	
	cellGMM,penb	2.16	0.04	0.20		2.41	0.05	0.23		2.63	0.04	0.19	
	MNM		0.02	0.09			0.02	0.10			0.02	0.09	
	MCNM	4.09	0.02	0.09		4.35	0.02	0.10		43.20	0.02	0.09	
	MtM	22.76	0.02	0.09		22.67	0.02	0.10		19.88	0.02	0.09	
	cellMCD	17.49	0.92	2.35		10.52	0.28	0.87		6.73	0.41	1.60	
	DI	1.44	0.05	0.27		4.64	0.13	0.49		1.45	0.09	0.67	
5	cellGMM,pen0	92.24	19.60	0.30	0.99	94.76	19.59	0.26	0.72	95.35	19.98	0.23	0.68
	cellGMM,penb	92.98	6.89	0.09	0.47	95.00	7.35	0.09	0.37	93.95	6.89	0.07	0.35
	MNM			0.70	1.14			0.64	0.94			0.95	1.54
	MCNM	94.12	20.51	0.69	1.38	92.42	20.41	0.62	1.10				
	MtM	99.54	37.85	0.67	1.33	99.34	37.11	0.63	1.09	93.93	48.76	0.79	1.38
	cellMCD	90.04	20.54	0.92	2.33	91.68	13.88	0.30	0.89	89.35	9.08	0.31	1.29
	DI	70.45	4.82	0.16	0.90	74.04	5.58	0.16	0.83	43.23	3.25	0.30	1.46
10	cellGMM,pen0	94.50	19.55	0.25	0.80	94.68	19.61	0.22	0.66	94.03	20.00	0.19	0.54
	cellGMM,penb	93.50	12.09	0.17	0.71	94.50	13.09	0.14	0.51	92.72	12.95	0.12	0.46
	MNM			0.94	1.52			0.71	1.02			1.30	1.98
	MCNM	91.16	35.64	0.94	1.68	84.56	33.59	0.77	1.24				
	MtM	97.84	46.95	0.88	1.66	91.82	44.90	0.74	1.19	79.41	54.32	1.06	1.69
	cellMCD	87.75	22.06	0.87	2.23	90.83	13.72	0.17	0.55	86.04	11.77	0.27	1.13
	DI	68.03	8.07	0.29	1.26	73.09	9.17	0.26	1.11	41.71	4.79	0.47	1.90

2.2 More extreme outliers

The last three scenarios replicate Scenarios 1-3 of the paper, with 5% and 10% of outliers randomly drawn from a uniform distribution in the wider interval $[-100, 100]$ without any additional constraints. Looking at Tables 5-7, it is evident that the model-based clustering methodologies with heavy-tailed distributions and non-robust GMM break down. Generally, we can deduce similar conclusions to the three scenarios reported in the paper, although those illustrated here demonstrate the advantage of cellGMM in handling more

extreme outliers.

Table 5: Number of samples on which each model can be properly computed (# samp.), mean of the Adjusted Rand Index and Misclassification Rate (mARI and mMR), Root Mean Squared Error of the posterior probabilities (RMSE_z), Mean Squared Error (MSE) of the prior probabilities and component mean vectors, and Kullback-Leibler (KL) discrepancy for the component covariance matrices per scenario, percentage of contamination, and model

		Scenario 1								
% out.	Model	# samp.	mARI	mMR	RMSE _z	MSE _z	MSE _{μ₁}	MSE _{μ₂}	KL _{Σ₁}	KL _{Σ₂}
5	celGMM.pen0	100	0.90	0.03	0.15	0.00	0.03	0.01	2.00	1.74
	celGMM.penb	100	0.94	0.01	0.10	0.00	0.02	0.01	0.52	1.97
	TCLUS	100	0.65	0.10	0.31	0.00	0.03	0.01	0.42	0.16
	schust_25	31	0.77	0.06	0.12	0.02	0.46	0.41	3.66	5.37
	schust_5	22	0.97	0.01	0.06	0.05	0.02	0.01	6.95	4.62
	MNM	98	0.00	0.37	0.61	0.03	122.46	17.44	25978.93	1938.54
	MCNM	96	0.00	0.35	0.59	0.03	128.69	1.71	18008.36	38.61
	MfM	96	0.00	0.35	0.59	0.03	70.74	0.84	25096.50	33.22
	10	celGMM.pen0	100	0.88	0.03	0.16	0.00	0.03	0.01	1.80
celGMM.penb		100	0.88	0.03	0.15	0.00	0.02	0.01	0.70	7.00
TCLUS		100	0.00	0.45	0.67	0.02	25.74	1.89	1813.74	171.52
schust_25		3	0.65	0.10	0.16	0.06	0.51	0.85	1.82	9.85
schust_10		3	0.96	0.01	0.09	0.06	0.01	0.03	5.33	6.77
MNM		100	0.00	0.38	0.62	0.04	397.69	6.20	23390.40	9198.86
MCNM		100	0.01	0.37	0.60	0.03	287.59	3.51	19187.35	712.23
MfM		100	0.02	0.38	0.61	0.02	140.47	1.71	22409.49	513.75
		Scenario 2								
% out.	Model	# samp.	mARI	mMR	RMSE _z	MSE _z	MSE _{μ₁}	MSE _{μ₂}	KL _{Σ₁}	KL _{Σ₂}
5	celGMM.pen0	100	0.55	0.13	0.31	0.00	0.09	0.04	2.90	1.90
	celGMM.penb	100	0.68	0.09	0.22	0.00	0.05	0.02	0.94	0.33
	TCLUS	100	0.54	0.13	0.33	0.00	0.04	0.02	0.64	0.23
	schust_25	0								
	schust_5	0								
	MNM	91	0.00	0.43	0.63	0.16	376.92	367.96	14768.24	3946.06
	MCNM	61	0.00	0.33	0.56	0.05	520.90	0.33	15285.74	1.76
	MfM	61	0.00	0.34	0.56	0.05	318.45	0.22	21295.98	2.07
	10	celGMM.pen0	100	0.54	0.14	0.31	0.01	0.10	0.06	2.62
celGMM.penb		100	0.58	0.12	0.27	0.01	0.10	0.04	1.28	0.55
TCLUS		100	0.00	0.45	0.66	0.02	16.12	1.14	1734.28	113.61
schust_25		0								
schust_10		0								
MNM		100	0.00	0.38	0.60	0.04	420.92	3.50	22776.54	9208.33
MCNM		100	0.00	0.37	0.59	0.02	311.45	0.35	19281.69	6.12
MfM		100	0.00	0.38	0.60	0.01	121.32	0.25	24329.24	14.83

Table 6: Number of samples on which each model can be properly computed (# samp.), mean of the Adjusted Rand Index and Misclassification Rate (mARI and mMR), Root Mean Squared Error of the posterior probabilities (RMSE_z), Mean Squared Error (MSE) of the prior probabilities and component mean vectors, and Kullback-Leibler (KL) discrepancy for the component covariance matrices per scenario, percentage of contamination, and model

		Scenario 3												
% out.	Method	# samp.	mARI	mMR	RMSE _z	MSE _π	MSE _{μ₁}	MSE _{μ₂}	MSE _{μ₃}	MSE _{μ₄}	KL _{Σ₁}	KL _{Σ₂}	KL _{Σ₃}	KL _{Σ₄}
5	cellGMM.pen0	100	0.98	0.01	0.04	0.00	0.02	0.02	0.01	0.01	8.77	8.75	8.11	8.06
	cellGMM.penb	100	0.98	0.01	0.03	0.00	0.01	0.01	0.01	0.01	3.00	5.80	4.54	3.41
	TCLUST	100	0.06	0.67	0.54	0.01	19.17	14.78	7.24	6.80	4869.17	4627.36	3015.07	2868.68
	sclust_25	0												
	sclust_5	3	0.97	0.01	0.03	0.36	0.01	0.01	0.01	0.04	14.15	34.78	21.14	42.83
	MNM	99	0.04	0.69	0.56	0.02	16.38	15.54	73.28	41.53	43294.77	37672.86	28185.69	25580.06
	MCNM	76	0.08	0.62	0.53	0.00	14.81	15.21	5.50	5.22	29392.59	22834.33	14466.93	10190.47
	MtM	76	0.19	0.50	0.51	0.00	12.23	7.43	1.71	2.55	24328.42	10921.84	3658.04	3148.88
10	cellGMM.pen0	100	0.96	0.01	0.08	0.00	0.02	0.02	0.01	0.01	7.80	7.68	6.68	6.61
	cellGMM.penb	100	0.95	0.02	0.07	0.00	0.01	0.01	0.01	0.01	3.59	29.71	23.71	16.16
	TCLUST	100	0.00	0.71	0.59	0.01	15.48	14.74	9.26	8.63	14352.00	14228.68	14224.02	14371.03
	sclust_25	0												
	sclust_10	0												
	MNM	76	0.01	0.71	0.59	0.03	190.67	158.03	138.34	41.71	46518.89	47563.60	39112.22	47922.68
	MCNM	57	0.00	0.70	0.59	0.02	164.63	187.70	8.53	16.81	37638.43	33529.67	20861.38	21787.61
	MtM	62	0.02	0.68	0.58	0.01	107.92	76.23	7.65	11.84	32409.38	28562.09	18241.94	19629.00

3 Real data examples: additional results

In this section, we provide additional results on the application of cellGMM to the real data sets illustrated in the paper.

Table 7: Statistics on outlier detection and imputation: percentage of True Positive and False Positive (%TP and %FP), Mean Absolute Error (MAE) and Root Mean Squared Error (RMSE) in comparing the original and imputed data matrices per scenario, percentage of contamination, and model

		Scenario 1				Scenario 2				Scenario 3			
% out.	Method	%TP	%FP	MAE	RMSE	%TP	%FP	MAE	RMSE	%TP	%FP	MAE	RMSE
5	cellGMM.pen0	98.92	21.11	0.22	0.58	98.86	21.11	0.20	0.48	99.37	21.09	0.23	0.61
	cellGMM.penb	98.94	3.92	0.10	0.53	98.76	5.05	0.10	0.43	99.16	4.24	0.08	0.41
	TCLUS	98.94	21.11			98.78	21.12			57.06	23.31		
	sclust_25	96.65	21.23										
	sclust_5	91.64	0.44							92.11	0.42		
	MCNM	57.19	10.19			75.31	13.81			40.01	15.03		
	MtM	63.83	37.28			72.72	34.10			79.59	40.78		
	cellMCD	98.68	13.78	0.52	1.46	98.68	2.18	0.04	0.21	98.74	3.94	0.23	1.14
DI	98.36	3.83	0.12	0.43	98.62	1.91	0.04	0.21	98.72	8.12	0.37	1.28	
10	cellGMM.pen0	98.58	16.82	0.23	0.66	98.92	16.79	0.20	0.49	99.21	16.75	0.23	0.68
	cellGMM.penb	98.55	6.10	0.19	0.80	98.83	6.77	0.16	0.57	98.96	5.90	0.15	0.66
	TCLUS	65.86	20.46			65.84	20.46			47.54	22.50		
	sclust_25	95.00	17.22										
	sclust_10	93.00	0.78										
	MCNM	70.77	22.93			70.96	23.04			47.14	25.09		
	MtM	71.25	35.34			71.59	33.87			71.00	47.06		
	cellMCD	98.72	13.41	0.53	1.47	98.82	1.96	0.06	0.24	98.61	2.84	0.18	0.93
DI	98.06	1.60	0.07	0.27	98.84	1.92	0.06	0.24	98.72	2.57	0.12	0.57	

3.1 Homogenized Meat Data Set

As for the simulation study, we report herein the ARI between the theoretical and the estimated clustering structure for cellGMM and the other competitors. From Table 8, it is evident that as the level of contamination increases, the performance of the rowwise and non-robust model-based clustering competitors dramatically decreases, whereas that of cellGMM diminishes less, remaining good. Additionally, Table 9 depicts the average classification results for cellGMM (i.e. cellGMM.penb) when $G = 4$, i.e., chicken and

Table 8: Adjusted Rand Index comparing the theoretical and the estimated classification of meat samples in two classes per model and percentage of contamination and missing values, i.e. $(a\%, b\%)$

	cellGMM	TCLUST	sclust	MNM	MCNM	MtM
(0%, 0%)	0.95	1.00	1.00	1.00	1.00	1.00
(3%, 0%)	0.95	0.86	0.85	0.81	0.80	0.75
(3%, 2%)	0.95	-	-	0.80	0.78	0.75
(10%, 0%)	0.93	0.45	0.73	0.48	0.25	0.36

Table 9: Average cellGMM classification results of the meat species with $G = 4$ and $G = 5$ (3% of contamination)

	1	2	3	4		1	2	3	4	5
Beef	0.97	0.00	0.00	0.03	Beef	0.97	0.03	0.00	0.00	0.00
Lamb	0.06	0.94	0.00	0.00	Lamb	0.12	0.88	0.00	0.00	0.00
Pork	0.00	0.00	0.82	0.18	Pork	0.13	0.00	0.78	0.04	0.05
Poultry	0.01	0.00	0.15	0.84	Chicken	0.21	0.00	0.02	0.75	0.02
					Turkey	0.05	0.00	0.00	0.85	0.10

turkey meats are considered in the same group representing poultry, and $G = 5$, both in the case of 3% of contamination. Although G is also set to 5, most of the chicken and turkey meats are grouped together, while the estimated cluster 5 contains few observations that are residual from the other clusters. The structure in four groups better distinguishes between the meat species, even if there is an “overlapping” between pork and poultry meats.

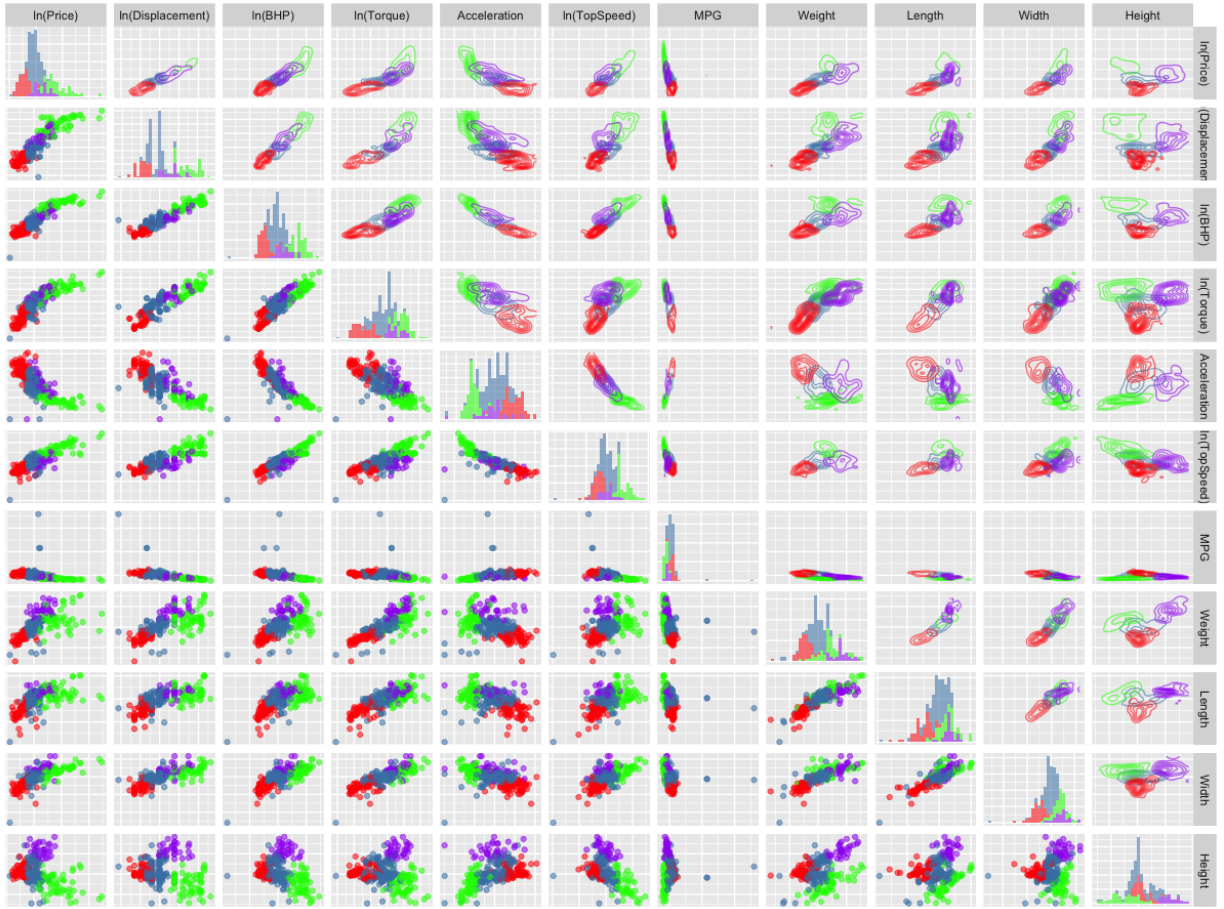


Figure 1: Pair plots of the Top Gear data set with the estimated classification in four groups (Cluster 1: blue; Cluster 2: red; Cluster 3: green; Cluster 4: purple)

3.2 Top Gear Data Set

The scatterplot for pairs of variables referring to the original, potentially contaminated data with the estimated classification in four groups is reported in Figure 1, while the full list of four clusters' classification is detailed below.

Cluster 1. Alfa Romeo Giulietta, Audi A3, Audi A4, Audi A4 Allroad, Audi A5, Audi A5 Sportback, Audi A6 Avant, Audi A6 Saloon, Audi Q3, Audi Q5, Audi TT Coupé, Audi TT Roadster, BMW 1 Series, BMW 1 Series Convertible, BMW 1 Series Coupé,

BMW 3 Series, BMW 3 Series Convertible, BMW 4 Series Coupé, BMW i3, BMW X1, BMW Z4, Caterham CSR, Caterham Super 7, Chevrolet Cruze, Chevrolet Orlando, Chevrolet Volt, Chrysler Delta, Citroen C4, Citroen C4 Picasso, Citroen C5, Citroen DS3, Citroen DS4, Citroen DS5, Dacia Duster, Fiat Bravo, Fiat Doblò, Fiat Punto Evo, Ford C-Max, Ford Focus, Ford Focus Estate, Ford Focus ST, Ford Kuga, Ford S-MAX, Honda Accord, Honda Civic, Honda CR-V, Honda CR-Z, Hyundai i40, Hyundai ix35, Hyundai Veloster, Jaguar XF, Jaguar XF Sportbrake, Jeep Compass, Kia Cee'd, Kia Optima, Kia Soul, Kia Sportage, Land Rover Freelander 2, Land Rover Range Rover Evoque, Lexus CT 200h, Lexus GS, Lotus Elise, Mazda CX-5, Mazda Mazda3, Mazda MX-5, Mercedes-Benz A-Class, Mercedes-Benz B-Class, Mercedes-Benz C-Class, Mercedes-Benz CLS Shooting Brake, Mercedes-Benz E-Class, Mercedes-Benz E-Class Coupé, Mercedes-Benz SLK, Mini Countryman, Mini Cooper, Mini John Cooper Works, Mini Roadster, Mitsubishi ASX, Mitsubishi Outlander, Morgan 3 Wheeler, Nissan Juke, Nissan Leaf, Nissan Qashqai, Nissan X-Trail, Peugeot 207 CC, Peugeot 3008, Peugeot 308, Peugeot 308 CC, Peugeot 308 SW, Peugeot 5008, Peugeot RCZ, Renault Mégane, Renault Scénic/Grand Scénic, Renault Twizy, SEAT Altea, SEAT León, Skoda Octavia, Skoda Yeti, Subaru BRZ, Subaru Forester, Subaru Legacy Outback, Subaru XV, Suzuki Grand Vitara, Toyota Avensis, Toyota GT 86, Toyota Prius, Toyota RAV4, Toyota Verso, Vauxhall Ampera, Vauxhall Astra, Vauxhall Astra GTC, Vauxhall Astra VXR, Vauxhall Cascada, Vauxhall Corsa VXR, Vauxhall Insignia, Vauxhall Insignia Sports Tourer, Vauxhall Mokka, Vauxhall Zafira, Vauxhall Zafira Tourer, Volkswagen Beetle, Volkswagen CC,

Volkswagen Eos, Volkswagen Golf, Volkswagen Golf Plus, Volkswagen Jetta, Volkswagen Passat, Volkswagen Scirocco, Volkswagen Tiguan, Volkswagen Touran, Volvo S60, Volvo S80, Volvo V40, Volvo V60, Volvo V70, Volvo XC70.

Cluster 2. Alfa Romeo MiTo, Aston Martin Cygnet, Audi A1, Chevrolet Aveo, Chevrolet Spark, Chrysler Ypsilon, Citroen C1, Citroen C3, Citroen C3 Picasso, Dacia Sandero, Fiat 500, Fiat 500 Abarth, Fiat 500L, Fiat Panda, Ford B-Max, Ford Fiesta, Honda Insight, Honda Jazz, Hyundai i10, Hyundai i20, Hyundai i30, Hyundai ix20, Kia Picanto, Kia Rio, Kia Venga, Mini Clubman, Mini Convertible, Mitsubishi i-MiEV, Mitsubishi Mirage, Nissan Micra, Nissan Note, Perodua MYVI, Peugeot 107, Peugeot 207 SW, Peugeot 208, Proton GEN-2, Proton Satria-Neo, Proton Savvy, Renault Clio, Renault Twingo, Renault Zoe, SEAT Mii, SEAT Toledo, Skoda Fabia, Skoda Roomster, Smart fortwo, Suzuki Alto, Suzuki Jimny, Suzuki Splash, Suzuki Swift, Suzuki Swift Sport, Suzuki SX4, Toyota Auris, Toyota AYGO, Toyota iQ, Toyota Yaris, Vauxhall Adam, Vauxhall Agila, Vauxhall Corsa, Vauxhall Meriva, Volkswagen Polo, Volkswagen Up.

Cluster 3. Aston Martin DB9, Aston Martin DB9 Volante, Aston Martin V12 Zagato, Aston Martin Vanquish, Aston Martin Vantage, Aston Martin Vantage Roadster, Audi A7 Sportback, Audi A8, Audi R8, Audi R8 V10, Audi RS4 Avant, Bentley Continental, Bentley Continental GTC, Bentley Flying Spur, Bentley Mulsanne, BMW 6 Series, BMW 6 Series Convertible, BMW 6 Series Gran Coupé, BMW 7 Series, BMW M3, BMW M6, Bugatti Veyron, Chevrolet Camaro, Chrysler 300C, Corvette C6, Ferrari 458, Ferrari California, Ferrari F12, Ferrari FF, Infiniti EX, Infiniti G37, Infiniti M,

Jaguar F-Type, Jaguar XFR, Jaguar XJ Series, Jaguar XK, Lamborghini Aventador, Lamborghini Gallardo, Lexus IS, Lotus Evora, Lotus Exige S, Maserati GranTurismo, Maserati Quattroporte, McLaren MP4-12C, Mercedes-Benz C63 AMG, Mercedes-Benz CL-Class, Mercedes-Benz CLS-Class, Mercedes-Benz E63 AMG, Mercedes-Benz SL 63, Mercedes-Benz SL-Class, Mercedes-Benz SLS, Morgan Aero, Morgan Roadster, Nissan 370Z, Noble M600, Pagani Huayra, Porsche 911, Porsche Boxster, Porsche Panamera, Rolls-Royce Ghost, Rolls-Royce Phantom, Rolls-Royce Phantom Coupé, Vauxhall VXR8, Volkswagen Phaeton.

Cluster 4. Audi Q7, BMW X3, BMW X5, BMW X6, Chevrolet Captiva, Chrysler Grand Voyager, Ford Galaxy, Hyundai i800, Hyundai Santa Fe, Infiniti FX, Jeep Grand Cherokee, Jeep Wrangler, Kia Sorento, Land Rover Defender, Land Rover Discovery 4, Land Rover Range Rover, Land Rover Range Rover Sport, Lexus RX, Mercedes-Benz G-Class, Mercedes-Benz GL-Class, Mercedes-Benz M-Class, Mercedes-Benz R-Class, Mercedes-Benz S-Class, Mitsubishi Shogun, Nissan Pathfinder, Porsche Cayenne, SEAT Alhambra, Ssangyong Rodius, Toyota Land Cruiser, Toyota Land Cruiser V8, Vauxhall Antara, Volkswagen Sharan, Volkswagen Touareg, Volvo XC60, Volvo XC90.

As highlighted in the paper, we analyze this data set via a cluster-oriented approach. However, not all the cars have a perfect assignment to the corresponding cluster. Some of them have a maximum a posteriori probability lower than 0.80, with a moderately high second probability. For instance, the Renault Twizy, Citroen DS3, Nissan Juke, and Volkswagen Golf Plus are assigned to Cluster 1 with probabilities of 0.57, 0.66, 0.71,

and 0.77, respectively, and to Cluster 2 with probabilities of 0.34, 0.34, 0.29, and 0.23, respectively. Meanwhile, the Lotus Elise is assigned to Cluster 1 with a probability of 0.67, despite having a 0.32 probability of being associated to Cluster 4. On the other hand, the Suzuki SX4 and Toyota Auris, which belong to Cluster 2 with probabilities 0.66 and 0.74, respectively, would be grouped with compact and mid-size sedans and crossovers (Cluster 1) as a second choice. Finally, the SEAT Alhambra, which belongs to Cluster 4 with a probability of 0.71, would be grouped secondarily with compact and mid-size sedans and crossovers. Cluster 3, on the other hand, has assignment probabilities higher than 0.95.

References

- Cuesta-Albertos, J. A., A. Gordaliza, and C. Matran (1997). Trimmed k -means: An attempt to robustify quantizers. *The Annals of Statistics* 25(2), 553–576.
- Fritz, H., L. A. García-Escudero, and A. Mayo-Iscar (2012). tclust: An R package for a trimming approach to cluster analysis. *Journal of Statistical Software* 47(12), 1–26.
- Fritz, H., L. A. García-Escudero, and A. Mayo-Iscar (2013). A fast algorithm for robust constrained clustering. *Computational Statistics & Data Analysis* 61, 124–136.
- Ghahramani, Z., and M. I. Jordan (1994). Learning from incomplete data. Technical Report AI Lab Memo No. 1509, CBCL Paper No. 108, MIT AI Lab.
- Hubert, L., and P. Arabie (1985). Comparing partitions. *Journal of Classification* 2(1), 193–218.